IEEE Access
Multidisciplinary ⋮ Rapid Review ⋮ Open Access Journal

Received 19 April 2024, accepted 21 May 2024, date of publication 24 May 2024, date of current version 3 June 2024.

Digital Object Identifier 10.1109/ACCESS.2024.3405080

RESEARCH ARTICLE

An Enhanced Channel Estimation Scheme in OFDM-IM Systems With Index Pilots for IEEE 802.11p Standard

QING-SHANG DONG[1], SI-YU ZHANG[1,2], (Member, IEEE), BEHNAM SHAHRRAVA[3], (Member, IEEE), AND HUI ZHENG[1,4]

[1]School of Information and Communication Engineering, Beijing Information Science and Technology University, Beijing 100192, China
[2]Key Laboratory of Information and Communication Systems, Ministry of Information Industry, Beijing Information Science and Technology University, Beijing 100192, China
[3]Department of Electrical and Computer Engineering, University of Windsor, Windsor, ON N9B 3P4, Canada
[4]Key Laboratory of Modern Measurement and Control Technology, Ministry of Education, Beijing Information Science and Technology University, Beijing 100192, China

Corresponding author: Si-Yu Zhang (zhang1fs@bistu.edu.cn)

This work was supported in part by the National Natural Science Foundation of China (NSFC) under Grant 62301058, in part by the Research and Development Program of Beijing Municipal Education Commission under Grant 5212410922, and in part by Beijing High-Level Overseas Talents Returning to China Project under Grant 001.

ABSTRACT Orthogonal frequency division multiplexing with index modulation (OFDM-IM) is emerging as a robust technology, especially valued in vehicular communication scenarios for its resilience. In such dynamic environments, reliable channel estimation becomes critical to maintain system performance due to the fast time-varying and double dispersion channel nature. Despite the harsh conditions, OFDM-IM enhances system performance by leveraging inactive sub-carriers to convey additional information. However, these idle sub-carriers complicate channel estimation compared to traditional OFDM systems. In response to these challenges, this paper introduces an enhanced channel estimation scheme tailored for the IEEE 802.11p standard, which supports cooperative intelligent transport systems (C-ITS). Our proposed method, the enhanced time-domain reliable test frequency-domain interpolation with index pilots (E-TRFI-IP), strategically places pilots and utilizes the positions of inactive sub-carriers to facilitate accurate detection and prevent performance degradation from inadequate channel tracking. Additionally, to further improve channel estimation performance, a comparison threshold methodology for reliable sub-carriers test is introduced by utilizing the structure of IM and joint interpolation method. Extensive simulation results demonstrate that E-TRFI-IP significantly surpasses existing channel estimation methods for both OFDM and OFDM-IM in terms of channel estimation performance. Notably, OFDM-IM systems employing the E-TRFI-IP estimation scheme also exhibit superior performance in bit error rate (BER) compared to those using conventional OFDM-IM and other channel estimation techniques.

INDEX TERMS Channel estimation, orthogonal frequency division multiplexing (OFDM), index modulation (IM), time domain reliable test frequency domain interpolation (TRFI), IEEE 802.11p standard, vehicular communications.

I. INTRODUCTION

A. INTRODUCTION AND RELATED WORK

To facilitate the deployment of cooperative intelligent transportation systems (C-ITS), the IEEE 802.11p standard has been developed, focusing on the physical layer of wireless access in vehicular communication environments [1]. Given the doubly selective nature of such channels, orthogonal frequency division multiplexing (OFDM), despite its widespread use in 4G/5G communication systems, experiences significant performance degradation due to these channel conditions [2], [3], [4]. Consequently, OFDM with

The associate editor coordinating the review of this manuscript and approving it for publication was Olutayo O. Oyerinde.

Index Modulation (OFDM-IM), inspired by the principles of spatial modulation (SM) [5], has been introduced as a novel alternative for future 6G networks, aiming to address the inherent limitations of conventional OFDM [6], [7], [8]. In OFDM-IM systems, part of information is indicated by the status of sub-carriers and the rest of information is carried by modulated constellation symbols. Compared to traditional OFDM, OFDM-IM offers flexible spectral efficiency, improved peak-to-average power ratio (PAPR) [9], [10], and greater energy efficiency [11], [12], [13]. Furthermore, the use of inactive sub-carriers in OFDM-IM enhances its resistance to inter-carrier interference (ICI), rendering it an appealing choice for vehicular [14], [15] and high-speed railway (HSR) communications [16], [17].

Despite the notable advantages of OFDM-IM outlined previously, its practical implementation in vehicular communications encounters several challenges. Unlike traditional OFDM, OFDM-IM requires the detection of active sub-carrier indices to demodulate the index bits prior to the demodulation of constellation symbols. The majority of existing research assumes perfect channel state information (CSI) to facilitate this detection process [6], [18]. However, attaining perfect CSI in real-world scenarios, particularly in the context of vehicular communications, proves to be exceedingly challenging.

It is important to note that since OFDM-IM owns in-active (idle) sub-carriers, conventional channel estimation schemes for 802.11p in OFDM systems is not workable. Consequently, several channel estimation methods have been proposed specifically for OFDM-IM systems [19], [20], [21]. For instance, in [19], a least squares (LS) channel estimation approach utilizing some of the inactive sub-carriers for pilot signals was introduced. Additionally, channel estimation schemes that employ Zadoff-Chu sequences and the linear minimum mean squared error (LMMSE) algorithm were proposed in [20] and [21], respectively. However, these approaches have not adequately addressed the challenge of estimation in doubly-selective channels. In [22], the authors attempted to tackle this issue within OFDM-IM for vehicular communications by re-using the preambles of 802.11p and increasing the transmit power of active sub-carriers. Nevertheless, the corresponding works for OFDM-IM channel estimation in vehicular communication environments are still rare. Therefore, further investigation into robust channel estimation methods for OFDM-IM systems in such environments is still necessary.

In the domain of IEEE 802.11p-based vehicular communications, several channel estimation schemes for OFDM systems have been developed, providing a solid foundation for corresponding research in OFDM-IM systems. Notable existing channel estimation schemes for OFDM include spectral temporal averaging (STA) [23], constructed data pilot (CDP) [24], and time domain reliable test frequency domain interpolation (TRFI) [25]. The STA scheme leverages the temporal and frequency correlations among successive OFDM symbols to refine the channel estimates for the current symbol. The CDP scheme utilizes data sub-carriers as pilots and the correlation characteristics between each two adjacent symbols. In this way, the data sub-carriers from previous OFDM symbols are exploited to estimate the channel of the current symbol, thereby improving the accuracy of channel estimation. Nevertheless, recent research has indicated that the STA and CDP schemes may not sufficiently fulfill the requirements of advanced vehicle-to-everything (V2X) applications, in contrast to the more robust TRFI scheme [26]. This highlights the ongoing need for novel channel estimation strategies that can address the unique challenges posed by vehicular communication environments.

Drawing inspiration from Zhao et al. [24], the TRFI scheme utilizes previous received OFDM symbols to equalize the previous and current channel estimates and compare them with each other. Based on these comparisons, sub-carriers are classified into two categories: reliable sub-carriers (RS) and unreliable sub-carriers (URS). Channel estimates from reliable locations are then interpolated to the unreliable ones, thereby enhancing the accuracy of the channel estimation process. Building upon the conventional TRFI framework, Han et al. [27] introduced a modified TRFI estimator tailored for IEEE 802.11p OFDM systems. This enhanced scheme employs the Euclidean distance between received signals and constellation points to achieve superior estimation performance in environments with high signal-to-noise ratios (SNR). Given its demonstrated efficacy in V2X OFDM scenarios, the TRFI scheme presents a promising approach for channel estimation in OFDM-IM systems. Innovatively, a modified TRFI (M-TRFI) method specifically designed for IEEE 802.11p OFDM-IM systems was first proposed by Zhang et al. [22]. The M-TRFI approach re-utilizes preambles and LS techniques to compensate for missing information on inactive sub-carriers, significantly improving estimation performance in vehicular communication environments.

It is known that since the channels in vehicular communications are usually time-varying, necessitating channel tracking in most estimation schemes to achieve satisfactory performance. However, the presence of inactive sub-carriers in OFDM-IM complicates the channel tracking process significantly. Direct application of the TRFI scheme to OFDM-IM could consequently lead to severe performance degradation. The M-TRFI scheme attempts to solve this problem by replacing the current channel estimates with previous ones. This approach manages to deliver estimation performance comparable to that of conventional OFDM in scenarios with low to medium SNRs. However, in high SNR environments, the M-TRFI scheme experiences notable performance declines, particularly in terms of estimation accuracy and BER, largely due to the index bits detection errors.

B. CONTRIBUTIONS

In this paper, we propose an enhanced TRFI with index pilots (E-TRFI-IP) scheme to augment channel estimation

performance in OFDM-IM systems compliant with the IEEE 802.11p standard. Contrary to the channel estimation scheme presented in [22], the E-TRFI-IP leverages the inactive sub-carriers by inserting a sequence of pre-known pilots after index modulation. These pilots, termed as index pilots (IP), are positioned according to the index bits, converting the originally inactive sub-carriers into IP sub-carriers. Although these IP sub-carriers do not convey actual information data, they play a crucial role in channel tracking and channel estimation. Furthermore, to refine the channel estimation accuracy, a reliability test based on Euclidean distance (RTbED) [27] is applied to the E-TRFI-IP scheme. It is critical to note that the effectiveness of the RTbED relies on a dynamically determined threshold, the selection of which influences the overall performance of the E-TRFI-IP scheme. To identify an optimal threshold, extensive simulations were conducted across a variety of vehicular communication scenarios. Additionally, we have developed specific steps for updating RS within the E-TRFI-IP framework, tailored to the unique structure of OFDM-IM. Extensive simulation results demonstrate that the proposed E-TRFI-IP significantly outperforms existing channel estimation methods in both OFDM and OFDM-IM systems, delivering substantial improvements in terms of normalized mean squared error (NMSE) and BER across diverse vehicular communication environments.

Compared with the previous works, the main contributions of this paper can be summarized as follows:

- A novel E-TRFI-IP channel estimation scheme is proposed. In this scheme, inactive sub-carriers, as indicated by index bits, are utilized not only to convey implicit information but also to carry specially designed pilots. In this way, the proposed E-TRFI-IP scheme can have more RS, thereby enhancing the ability to track the channel and improve interpolation accuracy, which significantly improves the corresponding channel estimation performance.
- The architecture of OFDM-IM enables the proposed E-TRFI-IP scheme to utilize a greater number of pilots compared to existing schemes under the 802.11p standard. However, in the E-TRFI-IP scheme, pilots located on inactive sub-carriers may be prone to mis-detection due to the randomness of index bits and ambient noise, potentially compromising estimation performance. To address this challenge, this paper introduces a novel RS update method that leverages index pilots to enhance the reliability of RS, thereby improving the overall accuracy of channel estimation.
- Owing to the different vehicle mobility scenarios, the threshold parameters for updating RS are not consistent. Random selection of these thresholds can result in performance degradation. Consequently, to mitigate the adverse effects of inaccurate RS determination, extensive experiments are conducted across a range of vehicular communication scenarios. These experiments are designed to precisely calibrate the RS threshold, thereby minimizing the potential for performance loss.
- In addition, since new RS are obtained through the RS update method, inactive sub-carriers of OFDM-IM may appear in the extrapolation area of URS. Therefore, for OFDM-IM systems, only utilizing cubic interpolation like the conventional TRFI scheme may cause serious performance degradation. To solve this problem, in this paper, a joint interpolation and extrapolation method is presented, which avoids such performance loss.

The remainder of this paper is organized as follows: Section II describes the system model, including OFDM-IM and IEEE 802.11p standard specifications. Section III illustrates existing channel estimation schemes for IEEE 802.11p OFDM-IM systems. In Section IV, the concept of the proposed E-TRFI-IP scheme is introduced. The computational analysis is given in Section V. The performance of the proposed E-TRFI-IP scheme are verified and evaluated in Section VI through extensive simulation results. The conclusion is given in Section VII.

II. SYSTEM MODEL

In this section, the system model of OFDM-IM is first illustrated. Then, the IEEE 802.11p standard specification, frame structure and transceiver design are presented, respectively. Finally, the system model for channel estimation is described.

A. OFDM-IM

As an application of the index modulation in frequency domain, the difference between OFDM-IM and OFDM lies in that a portion of information is no longer simply mapped to constellations for transmission. Instead, it utilizes index sequences to indicate the active or inactive status of sub-carriers, which helps the system to carry a portion of the information. For OFDM-IM, the balance between energy efficiency (EE) and spectrum efficiency (SE) is achieved by flexibly adjusting the number of blocks, the number of sub-carriers each sub-block contained, and the quantities of activated sub-carriers across all sub-carriers. An OFDM-IM transmitter model is illustrated in Fig.1.

First, m bits $\mathbf{B}$ are split into G groups. Each group $\mathbf{B}_g$ contains p bits. K sub-carriers are divided into G sub-blocks, and each contains k available sub-carriers and u active sub-carriers, thus $m = pG$ and $K = kG$. p bits in each sub-block are divided into p_1 and p_2 bits, in other words, $p = p_1 + p_2$. p_1 and p_2 bits can be given by:

$$p_1 = \left\lfloor \log_2 C_k^u \right\rfloor, \quad p_2 = u \log_2 M, \tag{1}$$

where $\lfloor \cdot \rfloor$ is the floor operation, C_a^b represents the binomial coefficient and M is the constellation size.

For OFDM-IM, the mapping operation is not only performed by means of modulated symbols, but also by the indices of sub-carriers. The indices of u active sub-carriers are determined by a selection procedure based on the first p_1 bits of the incoming p-bit sequence for conveying additional information bits. The indices of u active sub-carriers in the

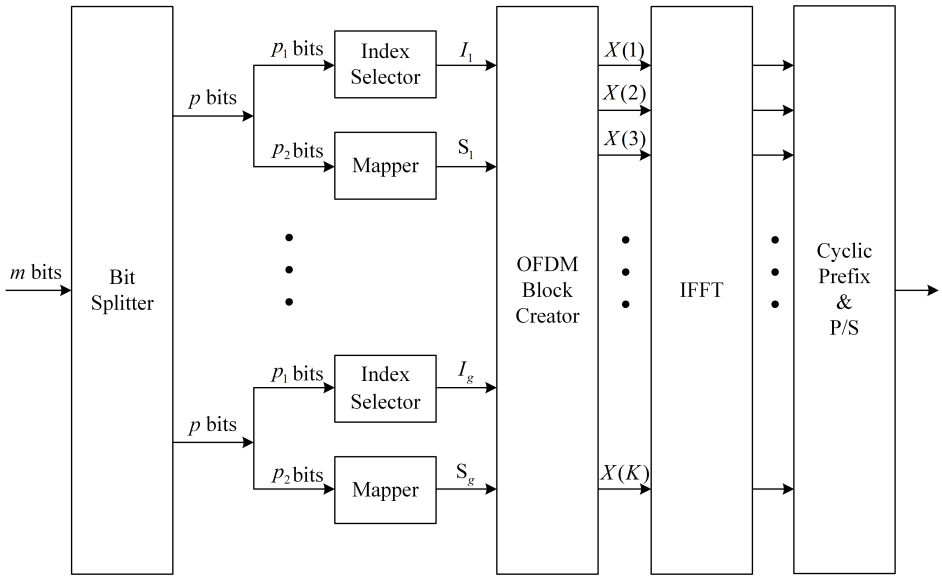

FIGURE 1. The system model of an OFDM-IM transmitter.

TABLE 1. A look-Up table of index modulation for $p_1 = 2$, $k = 4$, and $u = 2$.

Index Bits	Indices	Sub-blocks
[0, 0]	[1, 2]	[$S_g(1)$,$S_g(2)$,0,0]
[0, 1]	[1, 3]	[$S_g(1)$,0,$S_g(2)$,0]
[1, 0]	[2, 4]	[0,$S_g(1)$,0,$S_g(2)$]
[1, 1]	[3, 4]	[0,0,$S_g(1)$,$S_g(2)$]

g-th OFDM sub-block can be given by:

$$\mathbf{I}_g = \{i_{g,1}, i_{g,2}, \ldots, i_{g,u}\}, \tag{2}$$

where $i_{g,\gamma} \in \{1, \cdots, k\}$ for $1 \leq g \leq G$ and $1 \leq \gamma \leq u$. Furthermore, we represent the mapping of $\mathbf{I}_g$ corresponding to each sub-block g in the entire OFDM-IM block as $\mathcal{I}$.

An example of an index selector is given by Table. 1, where $p_1 = 2$, $k = 4$, and $u = 2$. For each sub-block, the indices of active sub-carriers are determined by the first two index bits, which could be [0, 0], [0, 1], [1, 0] and [1, 1]. Then, 2 index bits indicate the positions of active sub-carriers, which are denoted as $i_{g,\gamma}$. In Table. 1, 4 active sub-carrier combinations are illustrated, which are $i_{g,1} = [1, 2]$, $i_{g,2} = [1, 3]$, $i_{g,3} = [2, 4]$ and $i_{g,4} = [3, 4]$, respectively, while other sub-carriers carry no data and their values are usually set to 0.

After index modulation, in order to determine the data symbols transmitted over the u active sub-carriers, the p_2 bits are mapped to M-ary constellations and modulated to the u active sub-carriers according to the first p_1 bits. Therefore, the g-th constellation symbol block can be written as:

$$\mathbf{S}_g = [S_g(1), S_g(2), \ldots, S_g(u)], \tag{3}$$

where $S_g(\gamma) \in \chi_s$, and χ_s is the constellations.

Considering I_g and $\mathbf{S}_g$ for all G sub-blocks, a complete OFDM-IM sequence in frequency domain can be written as:

$$\mathbf{X} = [X(1), X(2), \ldots, X(K)]^T, \tag{4}$$

where $X(\alpha) \in \{0, \chi_s\}$, for $\alpha = 1, 2, \ldots, K$ and $(\cdot)^T$ denotes the transpose.

Thereafter, similar to OFDM, the baseband-equivalent OFDM-IM symbols are generated by applying the inverse fast Fourier transform (IFFT) operations. At OFDM-IM receiving side, p_1 bits need to be recovered at first through maximum likelihood (ML) or log-likelihood ratio (LLR) detections by deciding the status of sub-carriers. Then, the rest of p_2 bits can be recovered.

B. IEEE 802.11p STANDARD WITH OFDM-IM

IEEE 802.11p [1] standard is proposed and utilized in Internet of Vehicles (IoV) scenarios, including a number of enhancements required for C-ITS applications. IEEE 802.11p provides data exchange principles in vehicles to vehicles (V2V) and vehicles to infrastructures (V2I) applications. In order to cope with the rapid time-varying effects and multi-path delays in high-speed environments, IEEE 802.11p standard has made modifications in data link layer and physical layer from the traditional indoor communication protocols IEEE 802.11a.

Compared with IEEE 802.11a, the frequency bandwidth of IEEE 802.11p shrinks from 20MHz to 10MHz. Therefore, in 802.11p, the guard interval (GI) is also doubled. The GI of this scale can withstand root mean square (RMS) delay of hundreds of *ms* to reduce the impact of inter symbol interference (ISI) caused by multi-path transmissions. In addition, IEEE 802.11p usually utilizes OFDM with 64 sub-carriers, where 52 of them in the range from -26 to 26 are employed for information transmission. Sub-carriers

TABLE 2. IEEE 802.11p physical layer specifications.

Parameters	Values
Bandwidth	10 MHz
FFT size	64
FFT period	6.4μs
Guard interval duration	1.6μs
Symbol duration	8μs
Total sub-carriers	64
Pilot sub-carriers	4
Data sub-carriers	48
Null sub-carriers	12

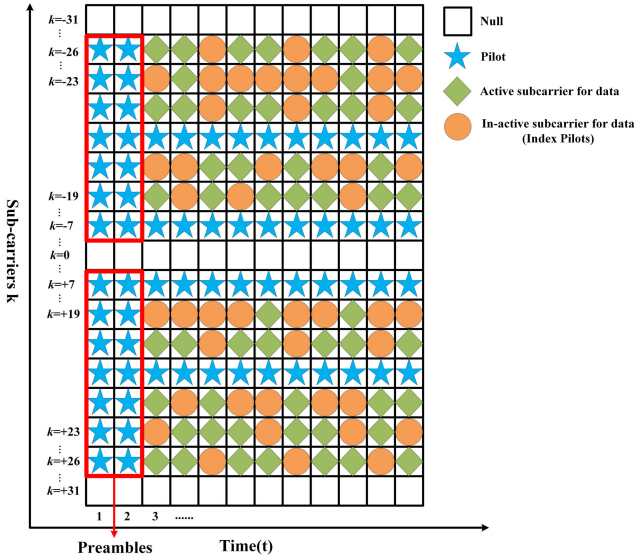

FIGURE 2. IEEE 802.11p sub-carriers arrangement for OFDM-IM.

with index -21, -7, 7, 21 are utilized for pilots, and the other sub-carriers are used for information transmission. Table. 2 illustrates the main physical layer parameters of IEEE 802.11p.

Fig.2 illustrates an IEEE 802.11p sub-carriers arrangement with OFDM-IM modulation. Compared with its OFDM counterpart, the corresponding OFDM-IM version has inactive sub-carriers which are usually zeros. However, different from the null positions specified by the IEEE 802.11p standard, the inactive sub-carriers in the frame of OFDM-IM implicitly conveys p_1 bits information through its position indices. The receiving side can recover the corresponding information by detecting these in-active sub-carriers.

A typical diagram of IEEE 802.11p transceiver utilizing OFDM-IM modulation is given in Fig.3. The generated bits are scrambled first to introduce a degree of randomness. After channel encoding and bits interleaving, the interleaved bits are systematically divided into index bits and constellation bits for OFDM-IM modulation. The index selector maps the index bits to a combination of active sub-carriers indices. The

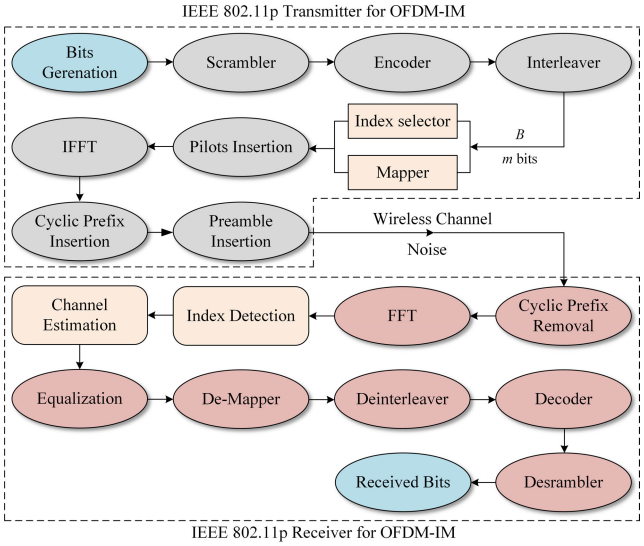

FIGURE 3. The diagram of an IEEE 802.11p transceiver.

rest bits are mapped to constellation symbols and placed on the corresponding activated sub-carriers. The bits mapping operation is succeeded by the construction of OFDM-IM symbols for transmission. Pilots and data symbols are assigned respectively according to the specification of IEEE 802.11p. Then, the frequency domain signals are processed through IFFT and CP insertion. Ultimately, an IEEE 802.11p frame can be formed by concatenating the constructed CP-OFDM-IM symbols with the predefined preambles.

Upon reaching the receiver, preambles serve the purposes of synchronization and channel estimation. Subsequent steps involve the removal of CP and FFT. Different from OFDM, before the channel estimation, OFDM-IM needs to obtain the indices of active sub-carriers, which are usually implemented through LLR detections. After, the pilot sub-carriers and the detected active indices are utilized for channel tracking and estimation. Then, the equalized data are de-mapped to retrieve the encoded bits. This is followed by deinterleaving, decoding, and descrambling operations in order to obtain the information bits.

C. SIGNAL MODELS FOR CHANNEL ESTIMATION

Assuming perfect synchronization, and ignoring the signal field, we focus on a frame that consists of two long preambles at the beginning followed by T OFDM-IM data symbols. Let $\mathcal{A}_{\text{on}}$ be the set of non-blank sub-carriers indices in Fig.2 with size A_{on}, the input-output relation between the transmitted and received OFDM-IM block ($\text{A}_{\text{on}} \times T$) can be written as:

$$\mathbf{Y}[\alpha, t] = \tilde{\mathbf{H}}[\alpha, t]\mathbf{X}[\alpha, t] + \mathbf{N}[\alpha, t], \alpha \in \mathcal{A}_{\text{on}}, \quad (5)$$

where $\mathbf{Y}[\alpha, t]$, $\mathbf{X}[\alpha, t]$, $\mathbf{N}[\alpha, t]$ are the transmitted OFDM-IM symbol, the received signal, and the noise with power N_0 of the α-th sub-carrier in the t-th OFDM-IM symbol, respectively. Here, $\tilde{\mathbf{H}}[\alpha, t]$ represents the time variant frequency response of the channel for all sub-carriers within

the transmitted frame. Then for simplicity, the transmitted symbols and the transmitted preambles can be written in vector form as follows:

$$\mathbf{y}_t[\alpha] = \tilde{\mathbf{h}}_t[\alpha]\mathbf{x}_t[\alpha] + \mathbf{n}_t[\alpha], \alpha \in \mathcal{A}_{\text{on}}, \tag{6}$$

$$\mathbf{y}_t^{(p)}[\alpha] = \tilde{\mathbf{h}}_t[\alpha]\mathbf{p}[\alpha] + \mathbf{n}_t^{(p)}[\alpha], \alpha \in \mathcal{A}_{\text{on}}, \tag{7}$$

where $\mathbf{x}_t[\alpha]$, $\tilde{\mathbf{h}}_t[\alpha]$ and $\mathbf{p}[\alpha]$ denote the t-th transmitted OFDM-IM symbol, the channel fading coefficients and the transmitted preamble in the frequency domain, respectively.

III. CONVENTIONAL CHANNEL ESTIMATION SCHEMES

In this section, we present a description of conventional channel estimation schemes for IEEE 802.11p standard. These schemes utilize the pilot sub-carriers and data sub-carriers of IEEE 802.11p to jointly perform channel estimation.

A. LS CHANNEL ESTIMATION SCHEME

LS is a classic and basic solution for channel estimation in IEEE 802.11p systems. For LS scheme, two received long preambles $\mathbf{y}_1^{(p)}[\alpha]$ and $\mathbf{y}_2^{(p)}[\alpha]$ are required to obtain the channel frequency response (CFR), which can be written as follows:

$$\hat{\tilde{\mathbf{h}}}_{\text{LS}}[\alpha] = \frac{\mathbf{y}_1^{(p)}[\alpha] + \mathbf{y}_2^{(p)}[\alpha]}{2\mathbf{p}[\alpha]}, \tag{8}$$

where $\mathbf{p}[\alpha]$ denotes the preknown symbols on the α-th sub-carriers of the long preambles, and $\hat{\tilde{\mathbf{h}}}_{\text{LS}}[\alpha]$ is the corresponding estimated CFR at the α-th sub-carriers.

LS algorithm only utilizes preambles to obtain channel estimates and assume the channel is time invariant, which reduces the estimation complexity. Also, since no data sub-carriers need to be considered, the LS scheme can be easily applied to OFDM-IM without significant modifications [19]. However, due to the time invariant assumption, the estimation accuracy of LS degrades with the increase of index bits. Therefore, the conventional LS algorithm cannot satisfy the requirement of vehicular communication environments.

B. INITIAL CHANNEL ESTIMATION SCHEME

Channel estimation in vehicular communications relies on the presumption of correlation among consecutive received symbols. To obtain a better estimation performance, the LS scheme is firstly conducted. Subsequently, an initial channel estimation [28] is employed to iteratively refine the estimates across all received symbols, as articulated in the following expression:

$$\mathbf{y}_{\text{eq}_t}[\alpha] = \frac{\mathbf{y}_t[\alpha]}{\hat{\tilde{\mathbf{h}}}_{\text{Initial}_{t-1}}[\alpha]}, \hat{\tilde{\mathbf{h}}}_{\text{Initial}_0}[\alpha] = \hat{\tilde{\mathbf{h}}}_{\text{LS}}[\alpha], \tag{9}$$

$$\hat{\tilde{\mathbf{h}}}_{\text{Initial}_t}[\alpha] = \frac{\mathbf{y}_t[\alpha]}{\mathbf{d}_t[\alpha]}, \tag{10}$$

where $\mathbf{y}_{\text{eq}_t}[\alpha]$ denotes the channel equalization value estimated previously for the t-th OFDM-IM symbol, and $\mathbf{d}_t[\alpha]$ is obtained by de-mapping the data sub-carrier $\mathbf{y}_{\text{eq}_t}[\alpha]$ to the nearest constellation point.

However, for OFDM-IM, since no data is carried on the inactive sub-carriers, $\mathbf{y}_{\text{eq}_t}[\alpha]$ can not be correctly de-mapped to $\mathbf{d}_t[\alpha]$, which stop the "initial channel estimation scheme" from being effectively applied in OFDM-IM systems.

C. TRFI BASED CHANNEL ESTIMATION SCHEMES

In order to alleviate the impact of de-mapping errors when updating channel estimates, the TRFI channel estimation scheme [25] is proposed. The main idea of TRFI is based on the frequency domain interpolation of the constructed reliable data pilots. The TRFI scheme is based on the results obtained from (8), (9), and (10), but it only employs the data sub-carriers within the received OFDM symbol. After obtaining the initial channel estimation $\hat{\tilde{\mathbf{h}}}_{\text{Initial}_t}[\alpha]$, by making use of the high temporal correlation between consecutive received OFDM symbols, the previously received OFDM symbols are equalized by $\hat{\tilde{\mathbf{h}}}_{\text{Initial}_t}[\alpha]$ and $\hat{\tilde{\mathbf{h}}}_{\text{TRFI}_{t-1}}[\alpha]$ respectively as follows:

$$\mathbf{y}'_{\text{eq}_{t-1}}[\alpha] = \frac{\mathbf{y}_{t-1}[\alpha]}{\hat{\tilde{\mathbf{h}}}_{\text{Initial}_t}[\alpha]},$$

$$\mathbf{y}''_{\text{eq}_{t-1}}[\alpha] = \frac{\mathbf{y}_{t-1}[\alpha]}{\hat{\tilde{\mathbf{h}}}_{\text{TRFI}_{t-1}}[\alpha]}. \tag{11}$$

The de-mapping results $\mathbf{d}'_{t-1}[\alpha]$ and $\mathbf{d}''_{t-1}[\alpha]$ can be obtained by utilizing the corresponding results of (11). Such de-mapping results are utilized to track and improve the channel estimate by defining two sub-carriers sets: RS set and URS set, which can be denoted as $\mathcal{S}_{\text{RS}}$ and $\mathcal{S}_{\text{URS}}$, respectively. The TRFI scheme utilizes the channel estimates at $\mathcal{S}_{\text{RS}}$ to interpolate the sub-carriers in $\mathcal{S}_{\text{URS}}$ based on the reliability test described in Algorithm 1.

Algorithm 1 TRFI Reliability Test Algorithm

Require: $\mathbf{d}'_{t-1}[\alpha]$ and $\mathbf{d}''_{t-1}[\alpha]$
  for all $\alpha \in \mathcal{A}_{\text{p}}$ **do**
    $\mathcal{S}_{\text{RS}} \longleftarrow \mathcal{S}_{\text{RS}} + \alpha$
  end for
  for all $\alpha \in \mathcal{A}_{\text{d}}$ **do**
    if $\mathbf{d}'_{t-1}[\alpha] == \mathbf{d}''_{t-1}[\alpha]$ **then**
      $\hat{\tilde{\mathbf{h}}}_{\text{TRFI}_t}[\alpha] = \hat{\tilde{\mathbf{h}}}_{\text{Initial}_t}[\alpha]$
      $\mathcal{S}_{\text{RS}} \leftarrow \mathcal{S}_{\text{RS}} + \alpha$
    else
      $\mathcal{S}_{\text{URS}} \leftarrow \mathcal{S}_{\text{URS}} + \alpha$
    end if
  end for
Output: $\mathcal{S}_{\text{RS}}$ and $\mathcal{S}_{\text{URS}}$

Here, $\mathcal{A}_{\text{p}}$ and $\mathcal{A}_{\text{d}}$ denote the indices sets of pilot and data sub-carriers, respectively. Since the four comb pilots are known in advance, the corresponding channel estimates for these sub-carriers are considered as reliable. For the data sub-carriers, a reliability test is applied, where the channel estimate at the α-th sub-carrier is considered reliable if $\mathbf{d}'_{t-1}[\alpha] = \mathbf{d}''_{t-1}[\alpha]$. Finally, frequency domain cubic

interpolation is applied by utilizing the channel estimates at $\mathcal{S}_{\mathrm{RS}}$ to recover the corresponding estimates at $\mathcal{S}_{\mathrm{URS}}$. Here, the interpolation function is denote as *cubic interpolation*$(\cdot)$. It is shown that cubic interpolation fits better than the linear one [25]. For the t-th OFDM symbol, the TRFI channel estimates of α-th sub-carrier are given as:

$$\hat{\hat{\mathbf{h}}}_{\mathrm{TRFI}_t}[\alpha] = \begin{cases} \hat{\hat{\mathbf{h}}}_{\mathrm{Initial}_t}[\alpha], & \alpha \in \mathcal{S}_{\mathrm{RS}}, \\ \textit{cubic interpolation}(\hat{\hat{\mathbf{h}}}_{\mathrm{TRFI}_t}[\mathcal{S}_{\mathrm{RS}}]), & \alpha \in \mathcal{S}_{\mathrm{URS}}. \end{cases} \tag{12}$$

Although the TRFI scheme is effective in OFDM systems, it cannot achieve channel-tracking in OFDM-IM systems due to the existence of inactive sub-carriers. Therefore, an M-TRFI is proposed for IEEE 802.11p OFDM-IM [22] to achieve the vehicular communication channel estimation task.

Since $\mathbf{y}_{\mathrm{eq}_t}[\alpha]$ needs to be de-mapped to $\mathbf{d}_t[\alpha]$ in (10), which is utilized for initial channel estimate, it is important to have an accurate $\mathbf{d}_t[\alpha]$. In OFDM-IM systems, the active sub-carriers are required to be de-mapped to the nearest constellation to obtain $\mathbf{d}_t[\alpha]$. However, the inactive sub-carriers are not able to be de-mapped correctly because no data are carried by these sub-carriers. Therefore, in M-TRFI scheme, if the α-th sub-carrier is inactive, $\hat{\hat{\mathbf{h}}}^{\text{M-TRFI}}_{\mathrm{Initial}_t}[\alpha]$ must be replaced by the CFR obtained by M-TRFI at the previous time, which can be written as:

$$\hat{\hat{\mathbf{h}}}^{\text{M-TRFI}}_{\mathrm{Initial}_t}[\alpha] = \begin{cases} \mathbf{y}_t[\alpha] \big/ \mathbf{d}_t[\alpha], & \text{if } \alpha \in \mathcal{A}_{\mathrm{p}}, \\ \hat{\hat{\mathbf{h}}}^{\text{M-TRFI}}_{t-1}[\alpha], & \text{if } \alpha \in \mathcal{A}_{\mathrm{null}}, \end{cases} \tag{13}$$

where $\mathcal{A}_{\mathrm{null}}$ denotes the indices set of inactive sub-carriers.

M-TRFI utilizes the previous CFR to replace the incorrect CFR on the inactive sub-carriers. Although this method achieves the first application of the TRFI algorithm in OFDM-IM systems, replacing the CFR blindly may bring serious performance degradation. This is because the distribution of inactive sub-carriers may be continuous, which leads to a widening gap between the replaced CFR and the actual CFR. Therefore, in this paper, an E-TRFI-IP channel estimation scheme is proposed, which is introduced in the next section.

IV. THE PROPOSED E-TRFI-IP CHANNEL ESTIMATION SCHEME

In this section, the concept of IP is described at first. Then, the proposed E-TRFI-IP channel estimation scheme is presented by introducing the RS update rule and the corresponding interpolation method.

First, the positions of IP at the transmitter need to be determined by the index bits. Then, IP insertion is implemented after the OFDM block creator, which is illustrated in the diagram of Fig.4. By detecting and utilizing these IP, the channel estimation can be achieved. Here, the set of IP is denoted as $\mathcal{M}_{\mathrm{IP}}$, which size is M_{IP}. After index modulation

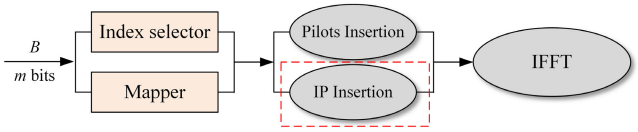

FIGURE 4. The diagram of IP insertion in IEEE 802.1p OFDM-IM transceiver.

and IP insertion, p_2 data bits are mapped according to a constellation set $\mathcal{M}_{\mathrm{c}}$, which size is M_{c}.

The EE of the proposed OFDM-IM structure can be represented by the number of bits transmitted per unit energy consumption. Quantitatively, EE is defined as the ratio of SE to the power consumed by an OFDM sub-carrier [29]. In order to compare the EE and SE among different OFDM based modulations, it is assumed that each symbol on a sub-carrier has unity power. Therefore, the EE of the conventional OFDM and the OFDM-IM with M-TRFI scheme can be written as:

$$\mathbf{EE}_0 = \frac{\mathbf{SE}}{u/k} = \frac{\lfloor \log_2 C_k^u \rfloor + u\log_2 M}{u} \text{bits/Joule}, \tag{14}$$

where u equals k in OFDM. For the OFDM-IM utilizing the proposed E-TRFI-IP scheme, compared with the conventional OFDM-IM, although the corresponding SE is unchanged, the EE may be compromised due to the IP insertion. The EE of E-TRFI-IP can be written as:

$$\mathbf{EE}_{\mathrm{IP}} = \frac{\mathbf{SE}}{(u+p_3)/k} = \frac{\lfloor \log_2 C_k^u \rfloor + u\log_2 M}{(u+p_3)} \text{bits/Joule}, \tag{15}$$

where p_3 denotes the number of IP in each sub-block. Table. 3 briefly introduces the SE and EE comparison among OFDM, OFDM-IM with M-TRFI [22] and OFDM-IM with E-TRFI-IP with variant M. It can be seen that when M is small, the EE of the OFDM-IM with E-TRFI-IP is the same as that of OFDM.

In order to effectively detect the index bits, the constellations from $\mathcal{M}_{\mathrm{IP}}$ and $\mathcal{M}_{\mathrm{c}}$ should be readily differentiable, thus $\mathcal{M}_{\mathrm{IP}} \cap \mathcal{M}_{\mathrm{c}} = \varnothing$. For example, if $M = 4$, $\mathcal{M}_{\mathrm{c}}$ could be $\left\{-\frac{\sqrt{2}}{2} - \frac{\sqrt{2}}{2}j, -\frac{\sqrt{2}}{2} + \frac{\sqrt{2}}{2}j, \frac{\sqrt{2}}{2} + \frac{\sqrt{2}}{2}j, \frac{\sqrt{2}}{2} - \frac{\sqrt{2}}{2}j\right\}$ and $\mathcal{M}_{\mathrm{IP}}$ could be $\{+1, -1, +j, -j\}$, which is shown in Fig.5.

At the receiving side, the indices of in-active sub-carriers need to be detected based on LLR detection methods. To reduce the corresponding complexity, inspired by [30], an LLR-based detector for the proposed E-TRFI-IP scheme is introduced. For the t-th OFDM-IM symbol, the LLR of the α-th sub-carrier can be written as:

$$\gamma_t[\alpha] = \ln\left(\frac{\sum_{a=1}^{\mathrm{M_c}} \Pr\left(\mathbf{x}_t[\alpha] = \mathcal{M}_{\mathrm{c}}(a) \,|\mathbf{y}_t[\alpha]\right)}{\sum_{b=1}^{\mathrm{M_{IP}}} \Pr\left(\mathbf{x}_t[\alpha] = \mathcal{M}_{\mathrm{IP}}(b) \,|\mathbf{y}_t[\alpha]\right)}\right). \tag{16}$$

It can be seen from (16) that the α-th sub-carrier is more likely to be a constellation symbol, if $\gamma_t[\alpha]$

TABLE 3. Comparison of SE and EE among different channel estimation schemes for $k = 4$, and $u = 2$.

Metrics / Schemes	SE(b/s/Hz)			EE(b/J)		
	$M = 2$	$M = 4$	$M = 16$	$M = 2$	$M = 4$	$M = 16$
OFDM	1	2	4	1	2	4
OFDM-IM	1	1.5	2.5	2	3	5
M-TRFI (OFDM-IM)	1	1.5	2.5	2	3	5
E-TRFI-IP (OFDM-IM)	1	1.5	2.5	1	1.5	2.5

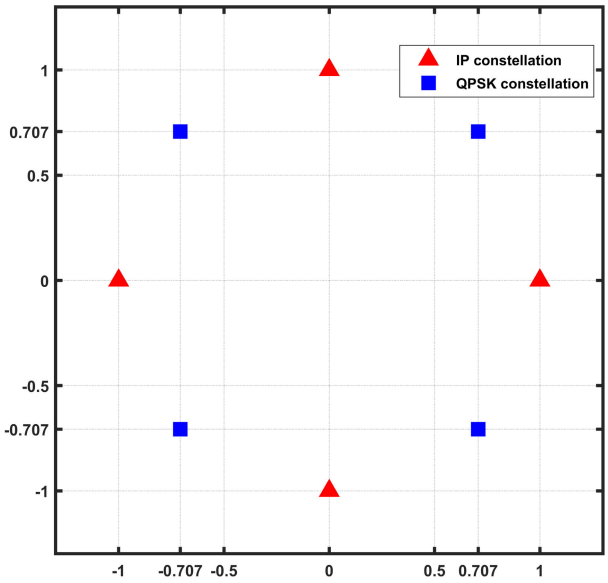

FIGURE 5. An illustration of IP constellation design for $\mathcal{M}_{\mathrm{IP}}$ and $\mathcal{M}_{\mathrm{c}}$ with M = 4.

is positive, and more likely to be an IP if $\gamma_t[\alpha]$ is negative. Since $\sum_{a=1}^{\mathrm{M_c}} \Pr\left(\mathbf{x}_t[\alpha] = \mathcal{M}_{\mathrm{c}}(a)\right) = k/u$ and $\sum_{b=1}^{\mathrm{M_{IP}}} \Pr\left(\mathbf{x}_t[\alpha] = \mathcal{M}_{\mathrm{IP}}(b)\right) = (u-k)/u$, using Bayes rule, (16) can be re-written as:

$$\gamma_t[\alpha] = \ln\left(\sum_{a=1}^{\mathrm{M_c}} \exp\left(-\frac{1}{N_0}\left|\mathbf{y}_t[\alpha] - \tilde{\mathbf{h}}_t[\alpha]\mathcal{M}_{\mathrm{c}}(a)\right|^2\right)\right) - \ln\left(\sum_{b=1}^{\mathrm{M_{IP}}} \exp\left(-\frac{1}{N_0}\left|\mathbf{y}_t[\alpha] - \tilde{\mathbf{h}}_t[\alpha]\mathcal{M}_{\mathrm{IP}}(b)\right|^2\right)\right) + \ln\left(\frac{k\mathrm{M_{IP}}}{(u-k)\mathrm{M_c}}\right). \tag{17}$$

To reduce the algorithm complexity and prevent numerical overflow, we write L_1 as:

$$L_1 = \ln\left(\sum_{a=1}^{\mathrm{M_c}} \exp\left(-\frac{1}{N_0}\left|\mathbf{y}_t[\alpha] - \tilde{\mathbf{h}}_t[\alpha]\mathcal{M}_{\mathrm{c}}(a)\right|^2\right)\right), \tag{18}$$

and L_2 as:

$$L_2 = \ln\left(\sum_{b=1}^{\mathrm{M_{IP}}} \exp\left(-\frac{1}{N_0}\left|\mathbf{y}_t[\alpha] - \tilde{\mathbf{h}}_t[\alpha]\mathcal{M}_{\mathrm{IP}}(b)\right|^2\right)\right). \tag{19}$$

In order to utilize Jacobian logarithm. Here, take the first term L_1 as an example, while the other term can be calculated in a similar way. We define $\delta_a = -\frac{1}{N_0}\left|\mathbf{y}_t[\alpha] - \tilde{\mathbf{h}}_t[\alpha]\mathcal{M}_{\mathrm{c}}(a)\right|^2$. Then, δ_a is utilized to re-write L_1 as:

$$\ln\left(\sum_{a=1}^{\mathrm{M_c}} e^{\delta_a}\right) = \ln\left(\sum_{a=1}^{(\mathrm{M_c}-1)} e^{\delta_a} + e^{\delta_{M_c}}\right) = \ln\left(e^{\ln\left(\sum_{a=1}^{(\mathrm{M_c}-1)} e^{\delta_a}\right)} + e^{\delta_{\mathrm{M_c}}}\right). \tag{20}$$

The further calculation of (20) can be written as [31], [32]:

$$\ln\left(e^A + e^B\right) = \max\{A, B\} + \ln\left(1 + e^{-|B-A|}\right). \tag{21}$$

With the assistant of (21), (20) can be written as:

$$\ln\left(\sum_{a=1}^{\mathrm{M_c}} e^{\delta_a}\right) = \max\left\{\ln\left(\sum_{a=1}^{(\mathrm{M_c}-2)} e^{\delta_a} + e^{\delta_{(\mathrm{M_c}-1)}}\right), \delta_{\mathrm{M_c}}\right\} + \ln\left(1 + e^{-\left|\delta_{\mathrm{M_c}} - \ln\left(\sum_{a=1}^{(\mathrm{M_c}-2)} e^{\delta_a} + e^{\delta_{(\mathrm{M_c}-1)}}\right)\right|}\right). \tag{22}$$

We note that if $\mathrm{M_c} > 2$, further calculations of (22) will become a recursive procedure. Both L_1 and L_2 can be obtained through the procedure, and the LLR value $\gamma_t[\alpha]$ can be obtained according to L_1 and L_2 through (17).

To demodulate the constellation symbols, the receiver needs to determine the positions of data sub-carriers by utilizing the active indices $\mathbf{I}_g$. Also, by concatenating $\mathbf{I}_g$ for every sub-block, $\mathcal{I}$ can be obtained, which is not only utilized for signal demodulation but also play an important role in the further channel estimation steps.

After obtaining the positions of in-active sub-carriers included in $\mathcal{I}$, the indices set of IP sub-carriers $\mathcal{A}_{\mathrm{IP}}$ can be obtained. Different from the conventional TRFI scheme, $\mathbf{d}_t[\alpha]$ can be written as:

$$\mathbf{d}_t[\alpha] = \begin{cases} \underset{\mathcal{M}_1}{\operatorname{argmin}}(|\mathbf{y}_{\mathrm{eq}_t}[\alpha] - \mathcal{M}_{\mathrm{c}}|^2), & \text{else}, \\ \mathbf{P}_t[\alpha], & \text{if } \alpha \in \mathcal{A}_{\mathrm{p}}, \\ \mathcal{M}_{\mathrm{IP}}[\alpha], & \text{if } \alpha \in \mathcal{A}_{\mathrm{IP}}, \end{cases} \tag{23}$$

where $\mathbf{P}_t[\alpha]$ are the predefined pilots of IEEE 802.11p standard, which are embedded to the sub-carriers $\{-21, -7, 7, 21\}$.

As shown in Fig.4, at the transmitting side, the predefined IP are inserted to the in-active sub-carriers. Therefore, as long as the positions of in-active sub-carriers are determined, the corresponding $\mathbf{y}_{\mathrm{eq}_t}[\alpha]$ can be de-mapped to $\mathcal{M}_{\mathrm{IP}}[\alpha]$. Then, the initial channel estimate $\hat{\tilde{\mathbf{h}}}_{\mathrm{Initial}_t}[\alpha]$ can be obtained through (10) and (23).

After having $\hat{\tilde{\mathbf{h}}}_{\mathrm{Initial}_t}[\alpha]$, the corresponding $\mathcal{S}_{\mathrm{RS}}$ and $\mathcal{S}_{\mathrm{URS}}$ can be obtained by (11) and Algorithm 1. We denote the $\mathcal{S}_{\mathrm{RS}}$ and $\mathcal{S}_{\mathrm{URS}}$ obtained in the initial step that need to updated as $\mathcal{S}^0_{\mathrm{RS}}$ and $\mathcal{S}^0_{\mathrm{URS}}$. Then, $\mathbf{y}'_{\mathrm{eq}_{t-1}}[\alpha]$ and $\mathbf{y}''_{\mathrm{eq}_{t-1}}$ are de-mapped to $\mathbf{d}'_{t-1}[\alpha]$ and $\mathbf{d}''_{t-1}[\alpha]$ according to (23). In the conventional TRFI scheme for OFDM, RS and URS are usually not accurate, especially when it applies to OFDM-IM systems, which significantly degrades the corresponding estimation performance. There are two reasons that cause the inaccuracy of $\mathcal{S}_{\mathrm{RS}}$ and $\mathcal{S}_{\mathrm{URS}}$, especially for OFDM-IM. First, the estimated active indices set $\mathcal{I}$ are not always perfect. Second, $\hat{\tilde{\mathbf{h}}}_{\mathrm{Initial}_t}[\alpha]$ obtained by incorrect $\mathbf{d}_t[\alpha]$ is usually inaccurate, which results in unreliable $\mathcal{S}_{\mathrm{RS}}$ and $\mathcal{S}_{\mathrm{URS}}$. Therefore, in this paper, a reliability test for $\mathcal{S}_{\mathrm{RS}}$ is introduced based on Euclidean distance. Here, the Euclidean distance between $\mathbf{y}_{\mathrm{eq}_t}[\alpha]$ and constellation symbol $\mathcal{M}_{\mathrm{c}}[k]$ can be written as:

$$\mathbf{D}^{\alpha}_t[q] = \left|\mathbf{y}_{\mathrm{eq}_t}[\alpha] - \mathcal{M}_{\mathrm{c}}[q]\right|^2, q = 1, \cdots, \mathrm{M_c}, \tag{24}$$

and the corresponding Euclidean distances set can be denoted as:

$$\mathcal{D} = \left\{\mathbf{D}^{\alpha}_t[q] : 1 \le q \le \mathrm{M_c}\right\}. \tag{25}$$

Then, in order to increase the reliability of $\mathbf{y}_{\mathrm{eq}_t}[\alpha]$, for the t-th OFDM-IM symbol, the ratio of the α-th sub-carrier between the minimum and the second minimum values in $\mathcal{D}$ is defined as:

$$\mathcal{T}^{\alpha}_t = \frac{\mathbf{D}^{\alpha}_t[q_1]}{\mathbf{D}^{\alpha}_t[q_2]}, \tag{26}$$

where $\mathbf{D}^{\alpha}_t[q_1]$ and $\mathbf{D}^{\alpha}_t[q_2]$ are the minimum and the second minimum distances in $\mathcal{D}$ respectively, and therefore $0 \le \mathcal{T}^{\alpha}_t \le 1$. Moreover, we define $\mathcal{S}^{\mathrm{p}}_{\mathrm{RS}}$ for an indices set of IP sub-carriers and pilot sub-carriers, which is considered reliable in the corresponding Euclidean distance test.

It can be seen from (26) that a small $\mathcal{T}^{\alpha}_t$ means that the distance from $\mathbf{y}_{\mathrm{eq}_t}[\alpha]$ to $\mathcal{M}_{\mathrm{c}}[q_1]$ is closer than the distance from $\mathbf{y}_{\mathrm{eq}_t}[\alpha]$ to $\mathcal{M}_{\mathrm{c}}[q_2]$. Then, the corresponding $\mathcal{S}_{\mathrm{RS}}$ can be regarded as reliable. On the contrary, if $\mathcal{T}^{\alpha}_t$ approaches 1, which means $\mathbf{y}_{\mathrm{eq}_t}[\alpha]$ has similar distance between $\mathcal{M}_{\mathrm{c}}[q_1]$ and $\mathcal{M}_{\mathrm{c}}[q_2]$, the corresponding $\mathcal{S}_{\mathrm{RS}}$ derived through $\mathcal{T}^{\alpha}_t$ should be considered unreliable.

Based on $\mathcal{T}^{\alpha}_t$, a threshold $\mathbf{T}_{th}$ can be defined to eliminate the unreliable $\mathcal{S}_{\mathrm{RS}}$ from $\mathcal{S}^0_{\mathrm{RS}}$. In the proposed method, the pilot sub-carriers in $\mathcal{S}^{\mathrm{p}}_{\mathrm{RS}}$ are known and reliable. Therefore, based on $\mathcal{S}^0_{\mathrm{RS}}$ and $\mathcal{S}^0_{\mathrm{URS}}$, subset $\mathcal{S}^0_{\mathrm{RS}'}$ and $\mathcal{S}^0_{\mathrm{URS}'}$ without the corresponding reliable indices in $\mathcal{S}^{\mathrm{p}}_{\mathrm{RS}}$ are defined, respectively. Then, for all α in $\mathcal{S}^0_{\mathrm{RS}'}$, if $\mathcal{T}^{\alpha}_t \le \mathbf{T}_{th}$, the α-th sub-carrier is regarded as reliable, and the corresponding α should be included in a new set $\mathcal{S}^1_{\mathrm{RS}}$. In contrast, if $\mathcal{T}^{\alpha}_t > \mathbf{T}_{th}$, the α-th sub-carrier in $\mathcal{S}^0_{\mathrm{RS}'}$ is regarded as unreliable. Hence, the corresponding α should be included in a new set $\mathcal{S}^1_{\mathrm{URS}}$. After considering all sub-carriers in $\mathcal{S}^{\mathrm{p}}_{\mathrm{RS}}$ and $\mathcal{S}^0_{\mathrm{URS}}$, the updated sets $\mathcal{S}^2_{\mathrm{RS}}$ and $\mathcal{S}^2_{\mathrm{URS}}$ can be obtained through (27):

$$\mathcal{S}^2_{\mathrm{RS}} = \left\{\mathcal{S}^1_{\mathrm{RS}} \cup \mathcal{S}^{\mathrm{p}}_{\mathrm{RS}}\right\}, \mathcal{S}^2_{\mathrm{URS}} = \left\{\mathcal{S}^1_{\mathrm{URS}} \cup \mathcal{S}^0_{\mathrm{URS}'}\right\}. \tag{27}$$

We note that the value of $\mathbf{T}_{th}$ can affect the channel estimation performance of the proposed E-TRFI-IP scheme. If the value of $\mathbf{T}_{th}$ is too small, the reliability of $\mathcal{S}^2_{\mathrm{RS}}$ may be compromised because the number of unreliable sub-carriers in $\mathcal{S}^0_{\mathrm{RS}'}$ that need to be updated to $\mathcal{S}^1_{\mathrm{URS}}$ may be insufficient. However, with a large $\mathbf{T}_{th}$, the size of $\mathcal{S}^2_{\mathrm{URS}}$ updated from $\mathcal{S}^0_{\mathrm{RS}'}$ may become larger than that of $\mathcal{S}^2_{\mathrm{RS}}$. It may affect the interpolation performance, which is the next step of the proposed channel estimation scheme. Therefore, a trade-off between $\mathcal{S}_{\mathrm{RS}}$ update and interpolation performance need to be made. In this paper, we pick the value of $\mathbf{T}_{th}$ through Monte Carlo simulations. The procedure of $\mathcal{S}_{\mathrm{RS}}$ and $\mathcal{S}_{\mathrm{URS}}$ update is described in Algorithm 2.

Algorithm 2 $\mathcal{S}_{\mathrm{RS}}$ and $\mathcal{S}_{\mathrm{URS}}$ Update Algorithm

Require: t, $\mathbf{T}_{th}$, $\mathbf{y}_{\mathrm{eq}_t}[\alpha]$, $\mathcal{S}^0_{\mathrm{RS}}$, $\mathcal{S}^0_{\mathrm{URS}}$ and $\mathcal{S}^{\mathrm{p}}_{\mathrm{RS}}$
  if $t = 1$ **then**
    $\mathcal{S}^0_{\mathrm{RS}_t} = \mathcal{S}^0_{\mathrm{RS}}, \mathcal{S}^0_{\mathrm{URS}_t} = \mathcal{S}^0_{\mathrm{URS}}$
  else
    $\mathcal{S}^0_{\mathrm{RS}_t} = \mathcal{S}^2_{\mathrm{RS}_{t-1}}, \mathcal{S}^0_{\mathrm{URS}_t} = \mathcal{S}^2_{\mathrm{URS}_{t-1}}$
  end if
  $\mathcal{S}^0_{\mathrm{RS}'} = \mathcal{S}^0_{\mathrm{RS}_t} - \mathcal{S}^{\mathrm{p}}_{\mathrm{RS}}$, $\mathcal{S}^0_{\mathrm{URS}'} = \mathcal{S}^0_{\mathrm{URS}_t} - \mathcal{S}^{\mathrm{p}}_{\mathrm{RS}}$
  for $\mathbf{y}_{\mathrm{eq}_t}[\alpha]$, $\alpha \in \mathcal{S}^0_{\mathrm{RS}'}$ **do**
    Having $\mathcal{T}^{\alpha}_t$ according to (24) and (26)
    if $\mathcal{T}^{\alpha}_t \le \mathbf{T}_{th}$ **then**
      $\mathcal{S}^1_{\mathrm{RS}} \longleftarrow \mathcal{S}^1_{\mathrm{RS}} + \alpha$
    else
      $\mathcal{S}^1_{\mathrm{URS}} \longleftarrow \mathcal{S}^1_{\mathrm{URS}} + \alpha$
    end if
  end for
  $\mathcal{S}^2_{\mathrm{RS}_t} = \{\mathcal{S}^1_{\mathrm{RS}} \cup \mathcal{S}^{\mathrm{p}}_{\mathrm{RS}}\}$, $\mathcal{S}^2_{\mathrm{URS}_t} = \{\mathcal{S}^1_{\mathrm{URS}} \cup \mathcal{S}^0_{\mathrm{URS}'}\}$
  $\mathcal{S}^2_{\mathrm{RS}} = \mathcal{S}^2_{\mathrm{RS}_t}, \mathcal{S}^2_{\mathrm{URS}} = \mathcal{S}^2_{\mathrm{URS}_t}$
Output: $\mathcal{S}^2_{\mathrm{RS}}$ and $\mathcal{S}^2_{\mathrm{URS}}$

We note that, different from the conventional TRFI scheme designed for OFDM, the step of producing $\mathcal{S}_{\mathrm{RS}}^{0}$ and $\mathcal{S}_{\mathrm{URS}}^{0}$ is only implemented when $t = 1$. When $t > 1$, Previous $\mathcal{S}_{\mathrm{RS}_{t-1}}^{2}$ and $\mathcal{S}_{\mathrm{URS}_{t-1}}^{2}$ are utilized in the reliability test. This step is regarded as the initial calculation of $\mathcal{S}_{\mathrm{RS}}^{0}$ and $\mathcal{S}_{\mathrm{URS}}^{0}$.

After $\mathcal{S}_{\mathrm{RS}}$ and $\mathcal{S}_{\mathrm{URS}}$ update, the frequency domain interpolation needs to be implemented in order to obtain the CFRs of the remaining unreliable sub-carriers. In the conventional TRFI based channel estimation scheme, only cubic interpolation is applied because there is no $\mathcal{S}_{\mathrm{RS}}$ and $\mathcal{S}_{\mathrm{URS}}$ update step in such schemes. For the proposed E-TRFI-IP channel estimation scheme, in-active sub-carriers of OFDM-IM for IP may appear in the extrapolation area of $\mathcal{S}_{\mathrm{URS}}$ due to the $\mathcal{S}_{\mathrm{RS}}$ and $\mathcal{S}_{\mathrm{URS}}$ update step. Therefore, taking these in-active sub-carriers into consideration, solely utilizing cubic interpolation may result in estimation performance degradation. Therefore, in this paper, cubic interpolation and linear extrapolation methods are jointly applied, which is given in Algorithm 3. We note that the analytical expression of the optimal extrapolation method is open for future research.

Algorithm 3 Joint Cubic Interpolation and Extrapolation Algorithm

Require: $\mathcal{S}_{\mathrm{RS}}^{2}$, $\mathcal{S}_{\mathrm{URS}}^{2}$, and $\mathbf{h}_{\mathrm{Initial}_t}$
  if $\max(\mathcal{S}_{\mathrm{URS}}^{2}) > \max(\mathcal{S}_{\mathrm{RS}}^{2})$ **then**
    $\mathcal{S}_{\mathrm{URS}}^{2,\mathrm{extra}} \longleftarrow \mathcal{S}_{\mathrm{URS}}^{2,\mathrm{extra}} + \max(\mathcal{S}_{\mathrm{URS}}^{2})$
  end if
  if $\min(\mathcal{S}_{\mathrm{URS}}^{2}) < \min(\mathcal{S}_{\mathrm{RS}}^{2})$ **then**
    $\mathcal{S}_{\mathrm{URS}}^{2,\mathrm{extra}} \longleftarrow \mathcal{S}_{\mathrm{URS}}^{2,\mathrm{extra}} + \min(\mathcal{S}_{\mathrm{URS}}^{2})$
  end if
  $\hat{\hat{\mathbf{h}}}_{\mathrm{IP}_t}[\mathcal{S}_{\mathrm{RS}}^{2}] = \hat{\hat{\mathbf{h}}}_{\mathrm{Initial}_t}[\mathcal{S}_{\mathrm{RS}}^{2}]$
  $\hat{\hat{\mathbf{h}}}_{\mathrm{IP}_t}[\mathcal{S}_{\mathrm{URS}}^{2,\mathrm{inter}}] = \mathit{cubic\ interpolation}(\hat{\hat{\mathbf{h}}}_{\mathrm{IP}_t}[\mathcal{S}_{\mathrm{RS}}^{2}])$
  $\hat{\hat{\mathbf{h}}}_{\mathrm{IP}_t}[\mathcal{S}_{\mathrm{URS}}^{2,\mathrm{extra}}] = \mathit{extrapolation}(\hat{\hat{\mathbf{h}}}_{\mathrm{IP}_t}[\mathcal{S}_{\mathrm{RS}}^{\mathrm{extra}}])$
Output: $\hat{\hat{\mathbf{h}}}_{\mathrm{IP}_t}$

Here, the extrapolation set of $\mathcal{S}_{\mathrm{URS}}^{2}$ and its complement are defined as $\mathcal{S}_{\mathrm{URS}}^{2,\mathrm{extra}}$, and $\mathcal{S}_{\mathrm{URS}}^{2,\mathrm{inter}}$, respectively. Then, the functions $\max(\cdot)$ and $\min(\cdot)$ represent the maximum and minimum index in $\mathcal{S}$, respectively. The *extrapolation*$(\cdot)$ is defined as the linear extrapolation function. $\mathcal{S}_{\mathrm{RS}}^{\mathrm{extra}}$ denotes the indices set for linear extrapolation, which includes $\mathcal{S}_{\mathrm{RS}}^{\mathrm{extra}}$ and $\mathcal{S}_{\mathrm{URS}}^{2,\mathrm{inter}}$. For the t-th OFDM-IM symbol, the estimated CFRs of the current α-th OFDM-IM symbol is written in (28). The diagram of the proposed E-TRFI-IP channel estimation process is illustrated in Fig.6.

$$\hat{\hat{\mathbf{h}}}_{\mathrm{IP}_t}[\alpha] = \begin{cases} \hat{\hat{\mathbf{h}}}_{\mathrm{Initial}_t}[\alpha], & \alpha \in \mathcal{S}_{\mathrm{RS}}^{2}, \\ \mathit{cubic\ interpolation}(\hat{\hat{\mathbf{h}}}_{\mathrm{IP}_t}[\mathcal{S}_{\mathrm{RS}}^{2}]), & \alpha \in \mathcal{S}_{\mathrm{URS}}^{2,\mathrm{inter}}, \\ \mathit{extrapolation}(\hat{\hat{\mathbf{h}}}_{\mathrm{IP}_t}[\mathcal{S}_{\mathrm{RS}}^{\mathrm{extra}}]), & \alpha \in \mathcal{S}_{\mathrm{URS}}^{2,\mathrm{extra}}. \end{cases} \tag{28}$$

V. COMPUTATIONAL COMPLEXITY ANALYSIS

In this section, we investigate the computational complexity of the proposed channel estimation schemes along with several existing alternatives. The evaluation of computational complexity is conducted by quantifying the number of real-valued operations required–specifically, multiplications/divisions and summations/subtractions–necessary for channel estimation in received OFDM-IM symbols. It is pertinent to note that our analysis pertains to complex-valued data. Within this context, a single complex-valued division entails six real-valued multiplications, two real-valued divisions, two real-valued summations, and one real-valued subtraction. Additionally, each complex-valued multiplication is accomplished using four real-valued multiplications and three real-valued summations.

The LS estimation is a fundamental technique in which the received preamble symbols are aggregated through summation, resulting in a total of $2\mathrm{A}_{\mathrm{on}}$ summations. Subsequently, the result of this summation is divided by the predefined preamble, necessitating an additional $2\mathrm{A}_{\mathrm{on}}$ divisions. Thus, the LS scheme requires a total of $2\mathrm{A}_{\mathrm{on}}$ summations and $2\mathrm{A}_{\mathrm{on}}$ divisions, respectively, to complete the estimation process.

The computational complexity of TRFI scheme mainly relies on the size of URS set. For the conventional TRFI, M-TRFI, and E-TRFI-IP schemes, the number of URS in each received symbol are defined as $\mathrm{A}_{\mathrm{URS}}^{\mathrm{TRFI}}$, $\mathrm{A}_{\mathrm{URS}}^{\mathrm{M\text{-}TRFI}}$, and $\mathrm{A}_{\mathrm{URS}}^{\mathrm{E\text{-}TRFI\text{-}IP}}$ respectively. Based on LS estimation, according to (9), (10), and (11), the TRFI scheme requires 4 extra complex-valued divisions. Moreover, TRFI utilizes the frequency domain interpolation to update the channel estimates. The cubic interpolation of one sub-carrier between two RS requires 26 multiplications/divisions and 30 summations/subtractions [28]. Therefore, the computational complexity of a conventional TRFI scheme is $34\mathrm{A}_{\mathrm{on}} + 26\mathrm{A}_{\mathrm{URS}}^{\mathrm{TRFI}}$ multiplications/divisions and $14\mathrm{A}_{\mathrm{on}} + 30\mathrm{A}_{\mathrm{URS}}^{\mathrm{TRFI}}$ summations/subtractions.

For the M-TRFI scheme, if the active sub-carriers detection of OFDM-IM is completed, compared with the conventional TRFI scheme for OFDM, the corresponding complexity of M-TRFI does not increase. Therefore, the computational complexity of M-TRFI is also $34\mathrm{A}_{\mathrm{on}} + 26\mathrm{A}_{\mathrm{URS}}^{\mathrm{M\text{-}TRFI}}$ multiplications/divisions and $14\mathrm{A}_{\mathrm{on}} + 30\mathrm{A}_{\mathrm{URS}}^{\mathrm{M\text{-}TRFI}}$ summations/subtractions.

As shown in Fig.6, the proposed E-TRFI-IP channel estimation scheme can be analyzed by dividing the scheme into two parts: the conventional TRFI procedure (part.A) and the E-TRFI-IP estimation procedure (part.B). It is worth noting that according to Algorithm 2, the complexity of part.A is only required to be counted when $t = 1$. Therefore, the computational complexity of part.A is $34\mathrm{A}_{\mathrm{on}}/T$ multiplications/divisions and $14\mathrm{A}_{\mathrm{on}}/T$ summations/subtractions. The part.B includes Euclidean distance reliability test, the cubic interpolation, and the linear extrapolation. These procedures have their own computational complexities. Here, we define the number of sub-carriers of performing the Euclidean distance reliability test and linear extrapolation

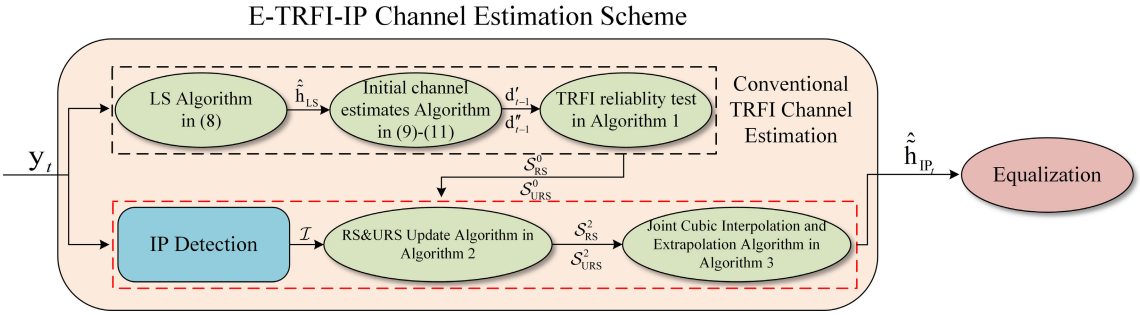

FIGURE 6. The diagram of the proposed E-TRFI-IP channel estimation scheme.

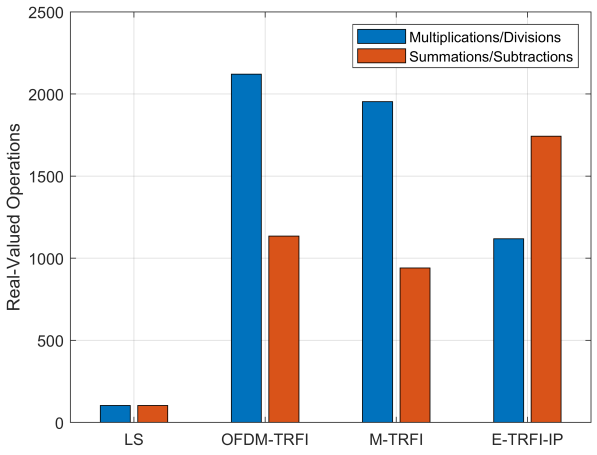

FIGURE 7. Computational complexity for different channel estimation schemes.

as A_{ED} and A_{ex}, respectively. According to (24) and (26), the Euclidean distance reliability test employs $A_{ED} + 2MA_{ED}$ real-valued divisions and $4MA_{ED}$ subtractions. Similar to the cubic interpolation, the linear extrapolation of one sub-carrier between two RS requires 8 multiplications/divisions and 8 summations/subtractions. Therefore, the total computational complexity of the proposed E-TRFI-IP scheme is $34/TA_{on} + (1 + 2M)A_{ED} + 26A_{URS}^{\text{E-TRFI-IP}} + 8A_{ex}$ multiplications/divisions, and $14/TA_{on} + 4MA_{ED} + 30A_{URS}^{\text{E-TRFI-IP}} + 8A_{ex}$ summations/subtractions.

Table.4 shows a detailed summary of the computational complexities for the studied estimators. In order to have a good approximation of the number of URS for different estimation schemes, we implement our 10000 times simulations. A detailed summary for the number of different URS in each received symbol is given in Table.5.

Fig. 7 shows a bar graph for the required multiplications/divisions, and summations/subtractions of the studied estimators. It can be noticed that, due to the initial calculations of $\mathcal{S}_{RS}^{0}$ and $\mathcal{S}_{URS}^{0}$, the proposed E-TRFI-IP reduces the overall computational complexity by 13% compared to the conventional TRFI scheme. Moreover, the proposed scheme even reduces the computational complexity of summations/subtractions by 89.6%.

VI. SIMULATION RESULTS

In this section, we present extensive simulation results for the proposed E-TRFI-IP channel estimation scheme in different vehicular communication scenarios. The proposed E-TRFI-IP scheme are compared with some existing schemes, including LS [19], TRFI [27] and M-TRFI [22]. We note that since the TRFI estimation scheme cannot work in OFDM-IM systems, thus OFDM needs to be applied to the conventional TRFI when comparing it with the proposed E-TRFI-IP scheme. The NMSE and BER performance of these channel estimation schemes is investigated and evaluated via simulations. Also, the impact of $\mathbf{T}_{th}$ on NMSE and BER performance in different scenarios is also considered.

In this section, a $G = 16$, $k = 4$, $u = 2$ OFDM-IM system with QPSK modulation is considered. The sub-carriers arrangement follows IEEE 802.11p standard. The value of IP are all set to 1 for simplicity. The vehicular channel models employed in this paper is then introduced in this section. After it, the selection of $\mathbf{T}_{th}$ is presented. Finally, the NMSE and BER performance of the proposed E-TRFI-IP channel estimation scheme is given and evaluated.

A. VEHICULAR CHANNEL MODELS AND MOBILITY

Vehicular channel models have been extensively investigated [33], [34], [35], and realistic vehicular channel models have been widely used in vehicular communication environments [36]. These models are obtained through channel measurements in the metropolitan of Atlanta, Georgia, USA. To evaluate the BER and NMSE performance of the proposed E-TRFI-IP scheme, very high, high, and low mobility vehicular environments are need to be considered, respectively. Therefore, in this paper, two vehicular channel models are chosen: (1) Vehicle-To-Vehicle Expressway Same Direction with Wall (VTV-SDWW). (2) VTV Urban Canyon (VTV-UC) [36]. VTV-UC is a channel scenario measured in Edgewood avenue in downtown Atlanta, where urban canyon characteristics exist. VTV-SDWW scenario is established on a highway with center wall between lanes. Based on these channel models, three scenarios with different speed are considered as follows:

TABLE 4. Computation complexity among different channel estimation schemes in terms of real-valued operations.

Estimation Scheme	Mul./Div.	Sum./Sub.
LS	$2\mathrm{A}_{\mathrm{on}}$	$2\mathrm{A}_{\mathrm{on}}$
TRFI	$34\mathrm{A}_{\mathrm{on}} + 26\mathrm{A}_{\mathrm{URS}}^{\mathrm{TRFI}}$	$14\mathrm{A}_{\mathrm{on}} + 30\mathrm{A}_{\mathrm{URS}}^{\mathrm{TRFI}}$
M-TRFI	$34\mathrm{A}_{\mathrm{on}} + 26\mathrm{A}_{\mathrm{URS}}^{\mathrm{M\text{-}TRFI}}$	$14\mathrm{A}_{\mathrm{on}} + 30\mathrm{A}_{\mathrm{URS}}^{\mathrm{M\text{-}TRFI}}$
E-TRFI-IP	$34/T\mathrm{A}_{\mathrm{on}} + (1+2M)\mathrm{A}_{\mathrm{ED}} + 26\mathrm{A}_{\mathrm{URS}}^{\mathrm{E\text{-}TRFI\text{-}IP}} + 8\mathrm{A}_{\mathrm{ex}}$	$14/T\mathrm{A}_{\mathrm{on}} + 4M\mathrm{A}_{\mathrm{ED}} + 30\mathrm{A}_{\mathrm{URS}}^{\mathrm{E\text{-}TRFI\text{-}IP}} + 8\mathrm{A}_{\mathrm{ex}}$

TABLE 5. The parameter values utilized in computation complexity (16QAM, SNR=0-15dB).

Parameter	$\mathrm{A}_{\mathrm{URS}}^{\mathrm{TRFI}}$	$\mathrm{A}_{\mathrm{URS}}^{\mathrm{M\text{-}TRFI}}$	$\mathrm{A}_{\mathrm{URS}}^{\mathrm{E\text{-}TRFI\text{-}IP}}$	A_{ED}	A_{ex}
Values	13.58	7.11	17.85	18.51	1.03

- Low mobility vehicular scenario, where the VTV-UC channel model is employed using V = 52 Kmph, which is equivalent to $\mathrm{F_d}$ = 300 Hz as a maximum Doppler shift.
- High mobility vehicular scenario, where the VTV-SDWW channel model with V = 104 Kmph and $\mathrm{F_d}$ = 600 Hz is employed.
- Very high mobility scenario, where the VTV-SDWW channel model is considered with V = 208 Kmph and $\mathrm{F_d}$ = 1200 Hz. This scenario is employed to further evaluate the robustness of the proposed schemes.

B. THE SELECTION OF $\mathbf{T}_{th}$

In this subsection, the value of $\mathbf{T}_{th}$ in different scenarios are selected by investigating the BER performance variation caused by using different $\mathbf{T}_{th}$. In order to conveniently demonstrate the influence of $\mathbf{T}_{th}$, we select five SNR values (0-50dB) at equal intervals, which are 5, 15, 25, 35, 45 as the reference SNRs.

Fig.8 shows that in low SNR scenarios (SNR≤15dB), by changing the value of $\mathbf{T}_{th}$, the corresponding BER is comparatively stable for all scenarios (Fig.8 (a), Fig.8 (b) and Fig.8 (c)). Nevertheless, it is clear that all scenarios have their own minimum BER values when SNRs are medium or high (SNR≥15dB). We calculate the average bit error rate of $\mathbf{T}_{th}$ at 5 different SNR scenarios, and utilize the $\mathbf{T}_{th}$ with the lowest value in the range 0.1 to 0.9 as the optimal $\mathbf{T}_{th}$. Simulation results show that in low, high, and very high mobility vehicular communication scenarios (Fig.8 (a), Fig.8 (b), and Fig.8 (c)), $\mathbf{T}_{th}$ = 0.25, 0.2, 0.15 can achieve the lowest average bit error rate 0.0789, 0.0798, and 0.0829, respectively.

C. NMSE AND BER PERFORMANCE

In this subsection, we provide and evaluate the NMSE and BER simulation results of the proposed E-TRFI-IP scheme in different scenarios utilizing the $\mathbf{T}_{th}$ values obtained in section VI-B. The definition of NMSE is given as follows:

$$\mathrm{NMSE_{IP}} = \sum_{t=1}^{T}\sum_{\alpha=1}^{A_{on}} \frac{\left|\tilde{\mathbf{h}}_t[\alpha] - \hat{\tilde{\mathbf{h}}}_{\mathrm{IP}_t}[\alpha]\right|^2}{\left|\tilde{\mathbf{h}}_t[\alpha]\right|^2}, \tag{29}$$

where $\tilde{\mathbf{h}}_t[\alpha]$ denotes the real channel coefficient, and $\hat{\tilde{\mathbf{h}}}_{\mathrm{IP}_t}$ denotes the estimated channel coefficient from the proposed E-TRFI-IP.

Fig.9 illustrates the performance of NMSE of the proposed scheme solely utilizing cubic interpolation and joint cubic interpolation and linear extrapolation method in low, high and very high mobility scenarios. Due to the RS update method, IP may appear in the extrapolation area of URS. Only utilizing cubic interpolation may result in the NMSE performance degradation, especially in low SNR (SNR<15dB) scenarios. In low mobility scenario, at NMSE = 10^0, the proposed joint cubic interpolation and linear extrapolation can achieve around 8dB performance gain compared to the scheme that only utilizing cubic interpolation. With the increment of SNRs, the gap gradually becomes smaller (around 2dB at NMSE = 10^{-3}) due to the low speed in the low mobility scenario. However, due to the high speed in the very high mobility scenario, even SNR increases, the amount of IP in the extrapolation area is still large, which cannot narrow the corresponding gap. Nevertheless, fig.9 shows that for the very high mobility scenario, at NMSE = 10^{-2}, the proposed joint cubic interpolation and linear extrapolation can still achieve around 10dB performance gain compared to its counterpart.

The impact of the number and modulation order of IP on the NMSE performance is analyzed in Fig.10 within a high mobility scenario. Reducing the number of IP can enhance the EE, yet it is shown in Fig.10 that reducing the number of IP to half (“HALF, IP = 1, QPSK”) compared to using all idle sub-carriers for IP (“FULL, IP = 1, QPSK”) significantly compromises the NMSE performance. Specifically, the NMSE at 2.4 × 10^{-3} for the full IP configuration exhibits a performance gain of approximately 22dB over the half IP setting. Despite this degradation, the performance of the half IP configuration still surpasses that of the conventional TRFI scheme in OFDM systems. This is attributed to the fact that when the number of IP continues to decrease until all IP are replaced by data, the proposed E-TRFI-IP scheme will degenerate to the conventional TRFI in OFDM systems. Further, Fig.10 explores the NMSE performance under varying constellation modulation orders.

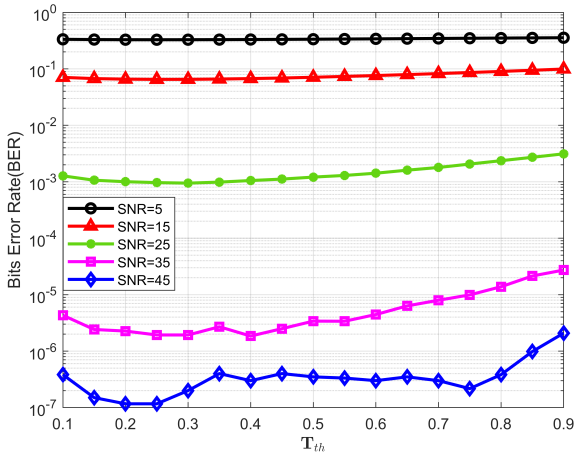

(a)

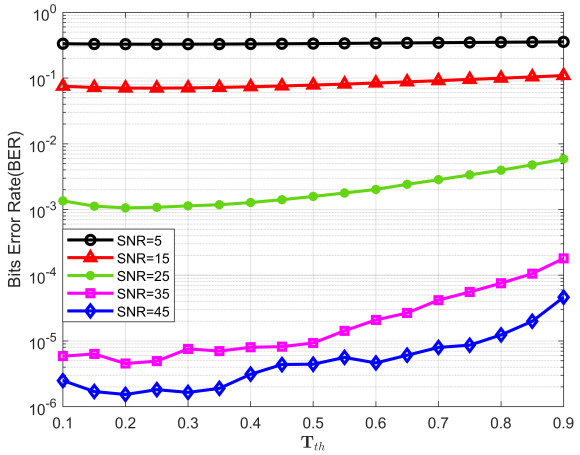

(b)

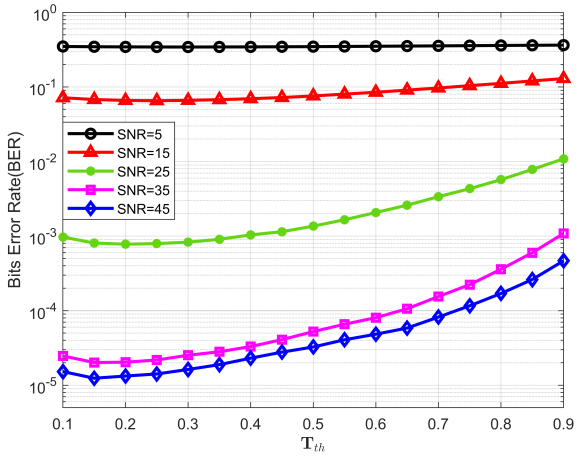

(c)

FIGURE 8. The performance of BER by utilizing different T_{th} values in (a) low mobility, (b) high mobility, and (c) very high mobility scenarios.

To mitigate detection errors, the IP value is increased to 2 for the 16QAM modulation scenario. This adjustment leads to substantial performance improvements in low to

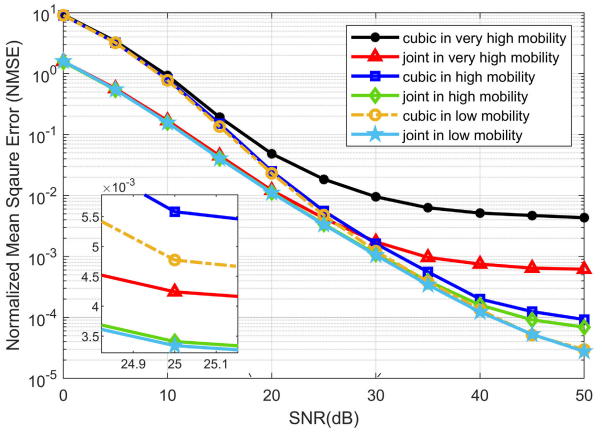

FIGURE 9. The NMSE performance of the proposed E-TFRI-IP scheme utilizing cubic interpolation and joint cubic interpolation and linear extrapolation method in low, high and very high mobility scenarios.

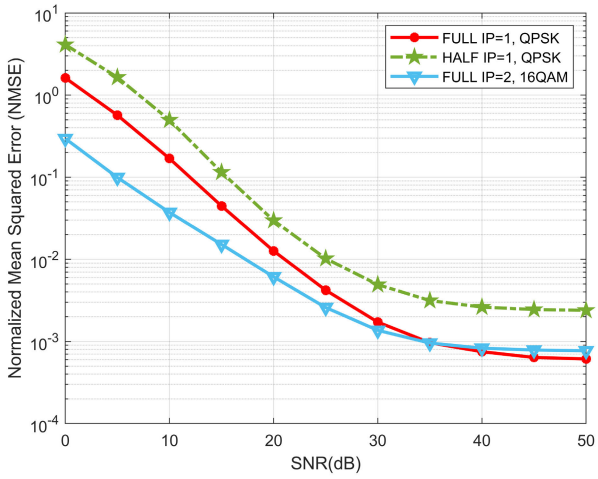

FIGURE 10. The NMSE performance of the proposed E-TFRI-IP scheme utilizing "FULL IP=1, QPSK", "FULL IP=1, QPSK" and "FULL IP=2, 16QAM" configurations in the very high mobility scenario.

medium SNR conditions (SNR<30 dB). For SNRs of 0 dB, 10 dB, 20 dB, and 30 dB, the performance enhancements for the "Full, IP=2, 16QAM" case are approximately 448%, 353%, 107%, and 26% respectively compared to the "FULL, IP=1, QPSK" scenario. In higher SNR environments (SNR>30 dB), the performance differential narrows due to the increased reliability of index bit detection.

The impact of the IP number and modulation order on BER performance is examined in Fig.11. This analysis follows observations of channel estimation performance degradation detailed in Fig.10. Specifically, the configuration of "FULL, IP=1, QPSK" significantly outperforms the "HALF, IP=1, QPSK" setting in terms of BER. For instance, at a BER of 1.5×10^{-4}, the "FULL, IP=1, QPSK" configuration exhibits approximately 21 dB higher performance gains compared to the "HALF, IP=1, QPSK" configuration. Moreover, due to more accurate channel estimations achieved in medium to low SNR scenarios, as shown in Fig.10,

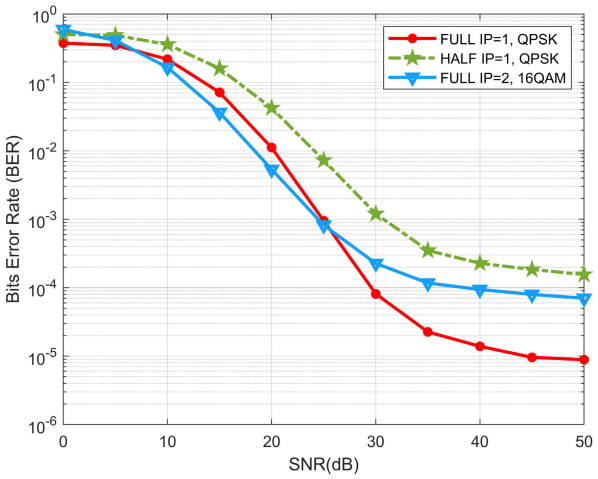

FIGURE 11. The BER performance of the proposed E-TFRI-IP scheme utilizing "FULL, IP=1, QPSK", "FULL, IP=1, QPSK" and "FULL, IP=2, 16QAM" configurations in the very high mobility scenario.

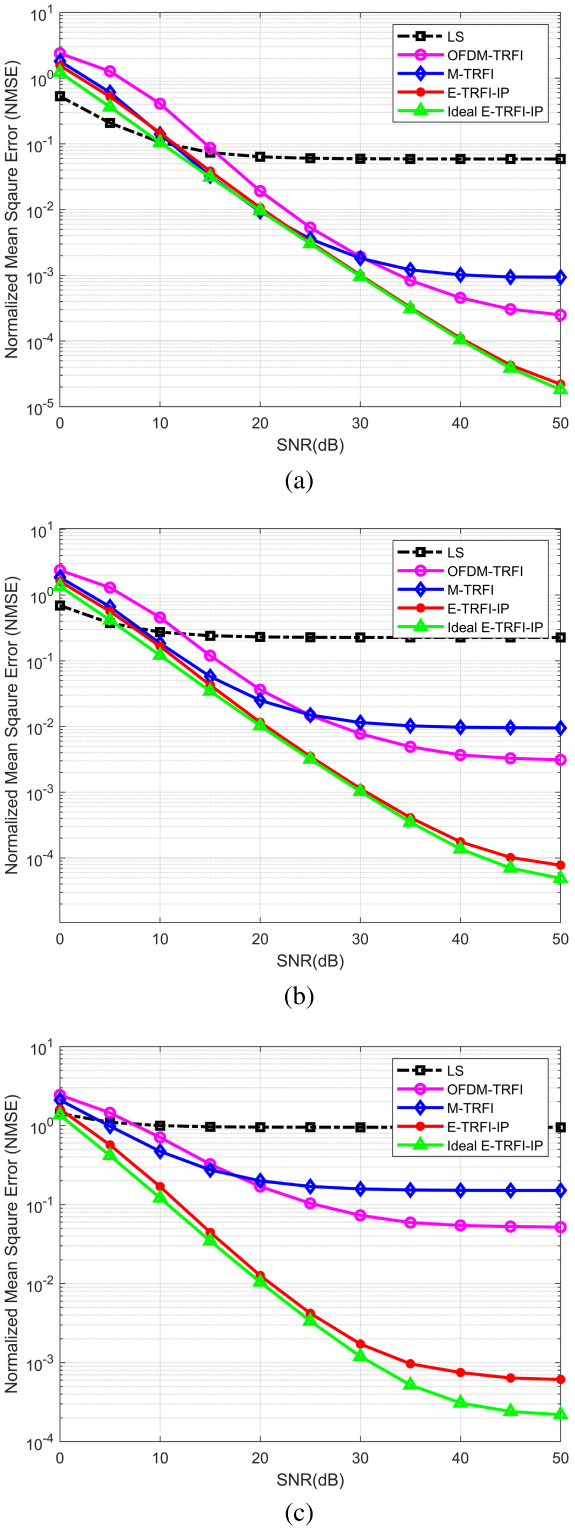

FIGURE 12. The NMSE performance comparisons among the proposed E-TRFI-IP scheme and existing channel estimation schemes in: (a) low mobility, (b) high mobility, and (c) very high mobility scenarios.

the BER performance when using 16QAM modulation is marginally better than with QPSK. However, at higher SNR levels, specifically above 25 dB, the BER performance for the 16QAM configuration starts to deteriorate relative to the QPSK system. For example, at a BER of 7×10^{-5}, the system employing QPSK modulation achieves around 19 dB better performance than the one using 16QAM.

Fig.12 illustrates the performance comparisons of NMSE among the proposed E-TRFI-IP scheme and existing channel estimation schemes, which include LS, TRFI and M-TRFI schemes. The comparisons are implemented in the low, high, and very high mobility scenarios, and the threshold values $\mathbf{T}_{th}$ are set to 0.25, 0.2, and 0.15, respectively. It is known that the proposed E-TRFI-IP scheme requires active sub-carriers detection before channel estimation, which may cause performance degradation due to detection errors. Therefore, we provide an ideal NMSE performance of the proposed E-TFRI-IP scheme, where all indices are assumed to be correctly detected, as a performance benchmark (denoted as "Ideal E-TRFI-IP"). According to Fig.12, the LS scheme achieves the worst performance because LS is ineffective in doubly-selective channels. M-TRFI owns significant performance improvement compared with the conventional LS in OFDM-IM. Nevertheless, due to the difficulties in channel tracking caused by in-active sub-carriers of OFDM-IM, M-TRFI suffers significant performance degradation, and becomes worse than that of TRFI in OFDM at medium to high SNR scenarios (SNR>20dB in the very high mobility scenario, SNR>25dB in the high mobility scenario, and SNR>30dB in the low mobility scenario). Thanks to the IP insertion, RS update process, and modified interpolation method, the proposed E-TRFI-IP scheme significantly outperforms other existing channel estimation schemes in high and very high mobility scenarios. For the low mobility scenario, at BER=2.5×10^{-4}, the proposed E-TRFI-IP scheme can also achieve around 14dB performance gains compared with the conventional TRFI in OFDM systems. Moreover, the proposed E-TRFI-IP can achieve a close

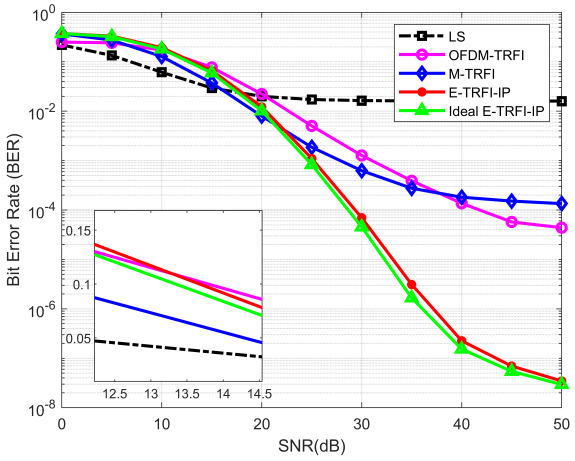

(a)

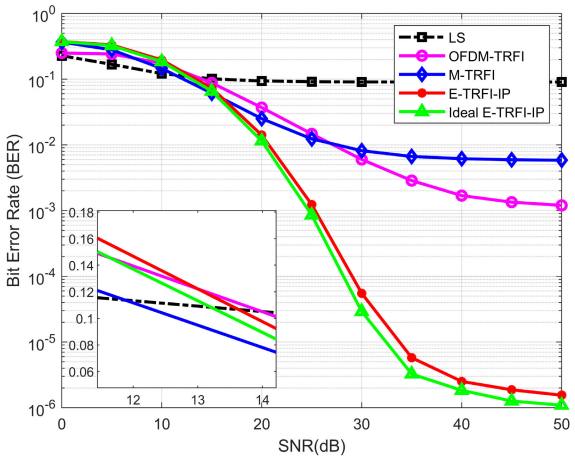

(b)

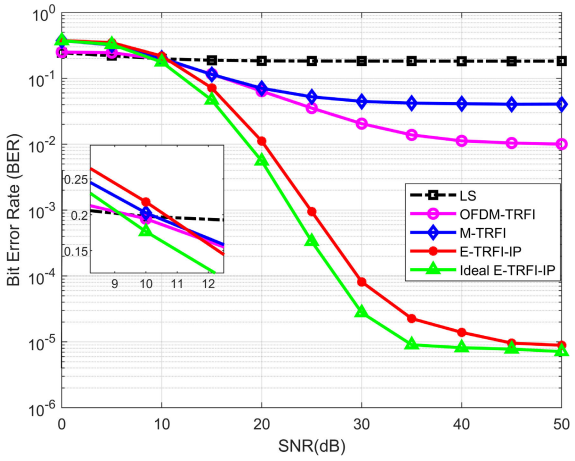

(c)

FIGURE 13. The BER performance comparisons of among the proposed E-TRFI-IP scheme and existing channel estimation schemes in: (a) low mobility, (a) high mobility, and (c) very high mobility scenarios.

performance to that of ''Ideal E-TRFI-IP'' by having a more accurate RS. Also, it can be seen that due to the different mobility in three vehicular communication scenarios, the overall NMSE performance in the low mobility scenario is the best, followed by that in the high mobility scenario, and the corresponding NMSE in very high mobility scenario is the worst.

Fig.13 shows the performance comparison of BER between among proposed E-TRFI-IP scheme and existing channel estimation schemes. Also, to facilitate evaluations, the BER performance of the proposed E-TRFI-IP, where all positions of IP are assumed to be correctly detected, is also provided, as a benchmark (denoted as ''Ideal E-TRFI-IP''). The BER comparisons are implemented in the low, high, and very high mobility scenarios, and the threshold values $\mathbf{T}_{th}$ are set to 0.25, 0.2, and 0.15, respectively. We know that OFDM-IM requires active sub-carriers detection before symbol demodulation. Therefore, the indices detection errors increase with the decrement of SNRs, which may cause performance loss. It is shown in Fig.13 that in low SNRs scenarios (SNR<14dB), the M-TRFI and the proposed E-TRFI-IP is slightly inferior to the LS and TRFI (for OFDM systems) schemes. However, it can be seen from Fig.13 that such gap is very small. With the increment of SNRs, the BER performance of the proposed E-TRFI-IP scheme significantly outperforms other existing schemes in different mobility scenarios. Also, the proposed E-TRFI-IP scheme can achieve a very close BER performance as that of the ''Ideal E-TRFI-IP'' case. In very high mobility scenarios, at BER=10^{-2}, the proposed E-TRFI-IP can achieve around 20dB performance gains compared with the conventional TRFI scheme. It is also worth noting that due to the different mobility in three vehicular communication scenarios, the overall BER performance in the low mobility scenario is the best, followed by that in the the high mobility scenario, and the corresponding BER in the very high mobility scenario is the worst. We can observe that the the conventional TRFI scheme is severely degraded when the channel becomes worse, whereas, the proposed E-TRFI-IP scheme reveals good robustness since compared with OFDM, OFDM-IM system has stronger anti-interference ability for the doubly dispersion channel. Therefore, the proposed E-TRFI-IP scheme is more robust than the conventional TRFI scheme.

VII. CONCLUSION

This article addresses the problem of channel estimation for OFDM-IM systems compliant with the IEEE 802.11p standard in vehicular communication environments. In this paper, we propose an E-TRFI-IP channel estimation scheme that incorporates a novel strategy for index pilot insertion, a reliability test for sub-carriers, and a joint interpolation method. By utilizing the above modifications and the distinctive structure of OFDM-IM, the proposed E-TRFI-IP scheme effectively improves the channel tracking ability and estimation performance. Additionally, a comparison threshold for updating reliable sets is introduced, and the optimal threshold values are determined for various vehicular communication scenarios. Extensive simulation results demonstrate that the E-TRFI-IP scheme achieves

robust performance across low, high, and very high mobility scenarios with NMSE improvements of up to 14 dB, 25 dB, and 35 dB, and BER improvements of up to 18 dB, 25 dB, and 30 dB, respectively. Consequently, the proposed E-TRFI-IP scheme markedly enhances channel estimation for OFDM-IM systems and outperforms existing conventional channel estimation methods for both OFDM and OFDM-IM systems.

REFERENCES

[1] D. Jiang and L. Delgrossi, "IEEE 802.11p: Towards an international standard for wireless access in vehicular environments," in *Proc. VTC Spring IEEE Veh. Technol. Conf.*, May 2008, pp. 2036–2040.
[2] N. A. Odhah, E. S. Hassan, M. I. Dessouky, W. E. Al-Hanafy, S. A. Alshebeili, and F. E. A. El-Samie, "Adaptive per-spatial stream power allocation algorithms for single-user MIMO-OFDM systems," *Wireless Pers. Commun.*, vol. 98, no. 1, pp. 1–31, Jan. 2018.
[3] N. A. Odhah, E. S. Hassan, M. Abdelnaby, W. E. Al-Hanafy, M. I. Dessouky, S. A. Alshebeili, and F. E. A. El-Samie, "Adaptive resource allocation algorithms for multi-user MIMO-OFDM systems," *Wireless Pers. Commun.*, vol. 80, no. 1, pp. 51–69, Jan. 2015.
[4] E. S. Hassan, "Multi user MIMO-OFDM-based power line communication structure with hardware impairments and crosstalk," *IET Commun.*, vol. 11, no. 9, pp. 1466–1476, Jun. 2017.
[5] R. Y. Mesleh, H. Haas, S. Sinanovic, C. W. Ahn, and S. Yun, "Spatial modulation," *IEEE Trans. Veh. Technol.*, vol. 57, no. 4, pp. 2228–2241, Jul. 2008.
[6] E. Basar, Ü. Aygölü, E. Panayirci, and H. V. Poor, "Orthogonal frequency division multiplexing with index modulation," *IEEE Trans. Signal Process.*, vol. 61, no. 22, pp. 5536–5549, Nov. 2013.
[7] H. Arslan, S. Dogan Tusha, and A. Yazar, "6G vision: An ultra-flexible perspective," *ITU J. Future Evolving Technol.*, vol. 1, no. 1, pp. 121–140, 2020.
[8] P. Yang, Y. Xiao, M. Xiao, and S. Li, "6G wireless communications: Vision and potential techniques," *IEEE Netw.*, vol. 33, no. 4, pp. 70–75, Jul. 2019.
[9] E. S. Hassan, "Performance enhancement and PAPR reduction for MIMO based QAM-FBMC systems," *PLoS ONE*, vol. 19, no. 1, Jan. 2024, Art. no. e0296999.
[10] H. Freag, E. S. Hassan, S. A. El-Dolil, and M. I. Dessouky, "New hybrid PAPR reduction techniques for OFDM-based visible light communication systems," *J. Opt. Commun.*, vol. 39, no. 4, pp. 427–435, Oct. 2018.
[11] E. Basar, M. Wen, R. Mesleh, M. Di Renzo, Y. Xiao, and H. Haas, "Index modulation techniques for next-generation wireless networks," *IEEE Access*, vol. 5, pp. 16693–16746, 2017.
[12] S.-Y. Zhang, B. Shahrrava, Y.-X. Zhang, and Z.-H. Zhuo, "A permutated partial transmit sequence scheme for PAPR reduction in polar-coded OFDM-IM systems," *IEEE Trans. Veh. Technol.*, vol. 72, no. 12, pp. 15867–15881, Jul. 2023.
[13] S.-Y. Zhang and H. Zheng, "PAPR reduction in OFDM-IM using dither signal sets," in *Proc. Int. Conf. Comput. Eng. Artif. Intell. (ICCEAI)*, Jul. 2022, pp. 275–278.
[14] H. Zhang, L.-L. Yang, and L. Hanzo, "LDPC-coded index-modulation aided OFDM for in-vehicle power line communications," in *Proc. IEEE 83rd Veh. Technol. Conf. (VTC Spring)*, May 2016, pp. 1–5.
[15] P. Yang, Y. Xiao, Y. L. Guan, M. Di Renzo, S. Li, and L. Hanzo, "Multidomain index modulation for vehicular and railway communications: A survey of novel techniques," *IEEE Veh. Technol. Mag.*, vol. 13, no. 3, pp. 124–134, Sep. 2018.
[16] H. Zhang, W. Li, and Y. Xu, "EM-based channel estimation with index modulation for high speed train communication," in *Proc. Int. Conf. Commun., Inf. Syst. Comput. Eng. (CISCE)*, Jul. 2019, pp. 390–394.
[17] Y. Cui and X. Fang, "Performance analysis of massive spatial modulation MIMO in high-speed railway," *IEEE Trans. Veh. Technol.*, vol. 65, no. 11, pp. 8925–8932, Nov. 2016.
[18] Z. Chen, Y. Lu, and S. G. Kang, "High-dimensional OFDM with in-phase/quadrature index modulation," *IEEE Access*, vol. 9, pp. 44198–44206, 2021.
[19] Y. Acar, S. A. Çolak, and E. BAŞAR, "Channel estimation for OFDM-IM systems," *Turkish J. Electr. Eng. Comput. Sci.*, vol. 27, no. 3, pp. 1908–1921, 2019.
[20] S. S. Mi, A. Siriwanitpong, P. Boonsrimuang, and P. Boonsrimuang, "Channel estimation for enhanced subcarrier index modulation OFDM using Zadoff-Chu sequence pilot in nonlinear channel," in *Proc. 19th Int. Conf. Electr. Eng./Electron., Comput., Telecommun. Inf. Technol. (ECTI-CON)*, May 2022, pp. 1–4.
[21] A. Kaplan, G. K. Kurt, I. Altunbas, U. Altun, F. A. Onaty, and D. Küçükyavuzy, "Impact of channel estimation on the performance of OFDM-IM with barrage jamming," in *Proc. 28th Signal Process. Commun. Appl. Conf. (SIU)*, Oct. 2020, pp. 1–4.
[22] S.-Y. Zhang, Q.-S. Dong, H. Zheng, Y.-X. Zhang, and B. Shahrrava, "Modified TRFI channel estimation scheme in OFDM-IM for 802.11p," in *Proc. IEEE 23rd Int. Conf. Commun. Technol. (ICCT)*, Oct. 2023, pp. 6–9.
[23] J. A. Fernandez, K. Borries, L. Cheng, B. V. K. V. Kumar, D. D. Stancil, and F. Bai, "Performance of the 802.11p physical layer in vehicle-to-vehicle environments," *IEEE Trans. Veh. Technol.*, vol. 61, no. 1, pp. 3–14, Jan. 2012.
[24] Z. Zhao, X. Cheng, M. Wen, B. Jiao, and C.-X. Wang, "Channel estimation schemes for IEEE 802.11p standard," *IEEE Intell. Transp. Syst. Mag.*, vol. 5, no. 4, pp. 38–49, Winter. 2013.
[25] Y.-K. Kim, J.-M. Oh, Y.-H. Shin, and C. Mun, "Time and frequency domain channel estimation scheme for IEEE 802.11p," in *Proc. 17th Int. IEEE Conf. Intell. Transp. Syst. (ITSC)*, Oct. 2014, pp. 1085–1090.
[26] G. Naik, B. Choudhury, and J.-M. Park, "IEEE 802.11bd & 5G NR V2X: Evolution of radio access technologies for V2X communications," *IEEE Access*, vol. 7, pp. 70169–70184, 2019.
[27] S. Han, J. Park, and C. Song, "Virtual subcarrier aided channel estimation schemes for tracking rapid time variant channels in IEEE 802.11p systems," in *Proc. IEEE 91st Veh. Technol. Conf. (VTC-Spring)*, May 2020, pp. 1–5.
[28] A. K. Gizzini, M. Chafii, A. Nimr, and G. Fettweis, "Deep learning based channel estimation schemes for IEEE 802.11p standard," *IEEE Access*, vol. 8, pp. 113751–113765, 2020.
[29] I. Sengupta, S. Dasgupta, and A. Das Barman, "Index and mode modulated orthogonal frequency division multiplexing with enhanced spectral efficiency," *Trans. Emerg. Telecommun. Technol.*, vol. 34, no. 4, p. e4735, Apr. 2023.
[30] T. Mao, Z. Wang, Q. Wang, S. Chen, and L. Hanzo, "Dual-mode index modulation aided OFDM," *IEEE Access*, vol. 5, pp. 50–60, 2017.
[31] J. Erfanian, S. Pasupathy, and G. Gulak, "Reduced complexity symbol detectors with parallel structure for ISI channels," *IEEE Trans. Commun.*, vol. 42, nos. 2–4, pp. 1661–1671, Feb. 1994.
[32] W. Koch and A. Baier, "Optimum and sub-optimum detection of coded data disturbed by time-varying intersymbol interference (applicable to digital mobile radio receivers)," in *Proc. IEEE Global Telecommun. Conf. Exhib.*, vol. 3, Dec. 1990, pp. 1679–1684.
[33] C.-X. Wang, X. Cheng, and D. I. Laurenson, "Vehicle-to-vehicle channel modeling and measurements: Recent advances and future challenges," *IEEE Commun. Mag.*, vol. 47, no. 11, pp. 96–103, Nov. 2009.
[34] X. Cheng, Q. Yao, M. Wen, C.-X. Wang, L.-Y. Song, and B.-L. Jiao, "Wideband channel modeling and intercarrier interference cancellation for vehicle-to-vehicle communication systems," *IEEE J. Sel. Areas Commun.*, vol. 31, no. 9, pp. 434–448, Sep. 2013.
[35] I. Sen and D. W. Matolak, "Vehicle-vehicle channel models for the 5-GHz band," *IEEE Trans. Intell. Transp. Syst.*, vol. 9, no. 2, pp. 235–245, Jun. 2008.
[36] G. Acosta-Marum and M. A. Ingram, "Six time- and frequency- selective empirical channel models for vehicular wireless LANs," *IEEE Veh. Technol. Mag.*, vol. 2, no. 4, pp. 4–11, Dec. 2007.

QING-SHANG DONG received the B.S. degree in engineering from Hainan University, in 2020. He is currently pursuing the M.S. degree with the School of Information and Communication Engineering, Beijing Information Science and Technology University (BISTU). His main research interests include 6G wireless networks, index modulation, channel estimation, OFDM-IM systems, and coding and information theory.

SI-YU ZHANG (Member, IEEE) received the Ph.D. degree in electrical and computer engineering from the University of Windsor, ON, Canada, in 2021. He is currently an Associate Professor with the School of Information and Communication Engineering, Beijing Information Science and Technology University (BISTU). His current research interests include beyond 5G techniques, OTFS and IM techniques, and coding and information theory, especially the design of polar decoders for 5G wireless networks.

BEHNAM SHAHRRAVA (Member, IEEE) received the Ph.D. degree in electrical engineering from the University of Waterloo, ON, Canada, in 1998. He is currently an Associate Professor with the Department of Electrical and Computer Engineering, University of Windsor. His research interests include advanced statistical and adaptive signal processing and their applications, primarily in wireless communications, multiuser detection, iterative decoding algorithms, and turbo receiver design.

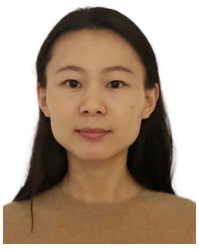

HUI ZHENG received the B.E. degree in communication engineering from PLA Information Engineering University, Zhengzhou, China, in 2011, and the M.E. and Ph.D. degrees in wireless communication systems from the University of Sheffield, Sheffield, U.K., in 2013 and 2019, respectively. She was a Postdoctoral Research Fellow with Ranplan Wireless Network Design Ltd., Cambridge, U.K., from February 2019 to March 2020. She is currently a Lecturer with the School of Information and Communication Engineering, Beijing Information Science and Technology University, Beijing, China. Her research interests include indoor ultra-dense networks, stochastic geometry, and channel modeling.